Am J Physiol Renal Physiol 320: F628–F643, 2021.
First published February 15, 2021; doi:10.1152/ajprenal.00505.2020

american physiological society

AMERICAN JOURNAL OF PHYSIOLOGY
RENAL PHYSIOLOGY

RESEARCH ARTICLE

Increased SGK1 activity potentiates mineralocorticoid/NaCl-induced kidney injury

Catalina Sierra-Ramos,[1] Silvia Velazquez-Garcia,[1,2] Ayse G. Keskus,[3] Arianna Vastola-Mascolo,[1] Ana E. Rodríguez-Rodríguez,[4] Sergio Luis-Lima,[2,4] Guadalberto Hernández,[1,2] Juan F. Navarro-González,[2,5] Esteban Porrini,[2,4] Ozlen Konu,[3,6,7] and Diego Alvarez de la Rosa[1,2]

[1]*Departamento de Ciencias Médicas Básicas, Universidad de La Laguna, La Laguna, Tenerife, Spain;* [2]*Instituto de Tecnologías Biomédicas, Universidad de La Laguna, La Laguna, Tenerife, Spain;* [3]*Interdisciplinary Neuroscience Program, Bilkent University, Ankara, Turkey;* [4]*Departamento de Medicina Interna, Universidad de La Laguna, La Laguna, Tenerife, Spain;* [5]*Unidad de Investigación y Servicio de Nefrología, Hospital Universitario Nuestra Señora de Candelaria, Santa Cruz de Tenerife, Spain;* [6]*Department of Molecular Biology and Genetics, Faculty of Science, Bilkent University, Ankara, Turkey; and* [7]*UNAM-Institute of Materials Science and Nanotechnology, Ankara, Turkey*

Abstract

Serum and glucocorticoid-regulated kinase 1 (SGK1) stimulates aldosterone-dependent renal Na^+ reabsorption and modulates blood pressure. In addition, genetic ablation or pharmacological inhibition of SGK1 limits the development of kidney inflammation and fibrosis in response to excess mineralocorticoid signaling. In this work, we tested the hypothesis that a systemic increase in SGK1 activity would potentiate mineralocorticoid/salt-induced hypertension and kidney injury. To that end, we used a transgenic mouse model with increased SGK1 activity. Mineralocorticoid/salt-induced hypertension and kidney damage was induced by unilateral nephrectomy and treatment with deoxycorticosterone acetate and NaCl in the drinking water for 6 wk. Our results show that although SGK1 activation did not induce significantly higher blood pressure, it produced a mild increase in glomerular filtration rate, increased albuminuria, and exacerbated glomerular hypertrophy and fibrosis. Transcriptomic analysis showed that extracellular matrix- and immune response-related terms were enriched in the downregulated and upregulated genes, respectively, in transgenic mice. In conclusion, we propose that systemically increased SGK1 activity is a risk factor for the development of mineralocorticoid-dependent kidney injury in the context of low renal mass and independently of blood pressure.

NEW & NOTEWORTHY Increased activity of the protein kinase serum and glucocorticoid-regulated kinase 1 may be a risk factor for accelerated renal damage. Serum and glucocorticoid-regulated kinase 1 expression could be a marker for the rapid progression toward chronic kidney disease and a potential therapeutic target to slow down the process.

aldosterone; chronic kidney disease; fibrosis; mineralocorticoid receptor; serum and glucocorticoid-regulated kinase 1

INTRODUCTION

Inappropriately increased mineralocorticoid receptor (MR) signaling plays an important role in the development of chronic kidney disease (CKD) (1). It has long been known that patients with primary aldosteronism develop hypertension and renal damage. Initially, renal damage was ascribed to increased blood pressure, but it has later been shown that these patients develop kidney injury to a larger extent than comparable individuals with primary hypertension (2). Extensive work on animal models supports a role for aldosterone excess and MR signaling in hypertension-dependent and -independent renal damage and the progression to CKD (1, 3, 4). Importantly, preclinical studies have conclusively shown a major role for MR antagonists in preventing or limiting kidney injury in a large variety of kidney disease models, including hypertension or diabetic nephropathy, glomerulonephritis, or the transition from acute kidney injury to CKD (3). These observations have been translated to humans, with data from clinical trials supporting the use of MR inhibition in limiting proteinuria and eliciting renoprotection (3).

The pathophysiological mechanisms involved in the deleterious effects of aldosterone/MR on the kidney expand beyond the role of this system in regulating tubular Na^+ reabsorption. MR expression has been detected not only in the distal nephron epithelium but also in podocytes, mesangial cells, endothelial and smooth muscle cells, interstitial fibroblasts, and macrophages (3). Activation of MR in these cell types has

Correspondence: D. Alvarez de la Rosa (diego.alvarez@ull.edu.es).
Submitted 18 September 2020 / Revised 1 February 2021 / Accepted 9 February 2021

been implicated in alterations in the renal circulation, oxidative stress, inflammation, glomerular and interstitial fibrosis, and alteration of the glomerular filtration barrier (1, 3, 4).

From a molecular perspective, aldosterone/MR-mediated kidney injury likely involves a multiplicity of direct and indirect mechanisms (3). MR is a nuclear receptor, and it is generally assumed that its main long-term effects are mediated by modulation of gene transcription. However, there is still an important knowledge gap about MR gene targets mediating the effects. One interesting candidate to mediate at least part of the processes leading to MR-induced kidney injury and the progression to CKD is serum and glucocorticoid-regulated kinase 1 (SGK1), a member of the AGC family of serine/threonine kinases. SGK1 is activated by insulin and several growth factors through the phosphatidylinositol 3-kinase pathway, involving downstream kinases 3-phosphoinositide-dependent kinase 1 and mammalian target of rapamycin complex 2 (5). SGK1 transcription and translation are tightly regulated, and its expression is enhanced by various stimuli including glucocorticoids and mineralocorticoids, being a direct target gene of both MRs and glucocorticoid receptors (6). The kinase regulates subcellular trafficking of many ion channels and transporters (7), at least in part by regulatory phosphorylation of the ubiquitin ligase neural precursor cell expressed developmentally down-regulated 4-like (NEDD4-2) (8, 9). SGK1 increases renal Na^+ reabsorption (10, 11) and K^+ excretion (12), thus participating in the control of blood pressure. *Sgk1* knockout protects mice against salt-induced hypertension in a high-fat diet context (13). Polymorphisms in the human *SGK1* gene have been linked to increased blood pressure (14), particularly associated with hyperinsulinemia (15), and the effects of dietary salt intake on blood pressure (16, 17). In addition, variants of SGK1 associate with insulin secretion (18) and type 2 diabetes (19). Consistently, SGK1 inhibition reduces blood pressure in hyperinsulinemic mice (20), and transgenic SGK1 activation potently induces hypertension in mice treated with a high-fat diet (21).

In addition to regulating transepithelial ion transport, SGK1 has further cellular functions through direct phosphorylation of signaling molecules such as glycogen synthase kinase-3β (GSK-3β) or transcription factors such as members of the FOXO family (22), a pathway that promotes cell survival and proliferation. SGK1 has been implicated in the development of inflammatory and fibrotic processes (23). Increased SGK1 expression has been described in kidney biopsies from patients with heavy proteinuria (24). Mice lacking SGK1 show decreased proteinuria and renal fibrosis in response to deoxycorticosterone acetate (DOCA)/NaCl treatment (25, 26), suggesting that this gene is key to develop kidney injury in response to excess mineralocorticoids. SGK1 has also been associated with aldosterone-induced oxidative stress and podocyte injury (27). SGK1 is also expressed in antigen-presenting cells (28) and is important during differentiation of T cells (29), playing a key role in salt-sensitive hypertension and renal inflammation (23, 28–30), which further supports a pleiotropic role for SGK1 in kidney disease.

Altogether, the available evidence suggests that increased systemic SGK1 activity could be a common factor underlying blood pressure-sensitive and -insensitive pathways leading to renal damage and thus accelerate the progression to CKD. To test this hypothesis, we took advantage of a transgenic mouse model (Tg.sgk1) previously developed in our laboratory using a modified mouse bacterial artificial chromosome (BAC) that drives the expression of a constitutively active mutant (SGK1-S422D) under its own promoter. This transgenic strain provides a model of generalized increase in SGK1 activity without overexpression of the kinase (21, 31, 32). We used a well-established model of mineralocorticoid excess and high NaCl intake in the context of uninephrectomy to induce hypertension and renal damage (33, 34). Our results show that transgenic mice displayed exacerbated glomerular hypertrophy, proteinuria, and fibrosis with a conserved glomerular filtration rate (GFR). We used transcriptomic analysis to define SGK1-modulated pathways in this model. In conclusion, we propose that systemically increased SGK1 activity could be a risk factor for the development of mineralocorticoid-dependent kidney injury in the context of low renal mass and independently of blood pressure changes.

METHODS

Ethics Statement/Study Approval

All experiments involving mice took place at the University of La Laguna. Animal procedures followed protocols previously approved by the University of La Laguna Ethics Committee on Research and Animal Welfare (permit no. CEIBA2016-0197) and were performed in accordance with European Community guidelines for the use of experimental animals (2010/63/EU) and with Spanish law for the protection of animals (RD53/2013).

Transgenic Expression of Constitutively Active SGK1 in Mice

The generation of transgenic mice expressing a constitutively active mutant of SGK1 (S422D) has been previously described (21, 31, 32). Briefly, a BAC containing 180 kb of mouse genomic DNA that includes the full SGK1 gene but no other known or predicted genes was obtained from the BACPAC Resources Center (Children's Hospital Oakland Research Institute, Oakland, CA) and modified by homologous recombination in *Escherichia coli* to add a constitutively activating point mutation (S422D). Founder animals harboring the transgene were backcrossed with C57BL/6 mice for eight generations. Mice homozygous for the transgene were obtained by crossing heterozygous animals.

Animal Procedures

Mice were kept on a 12:12-h light-dark cycle at 22°C with ad libitum access to food and water. Unilateral nephrectomy (NPX) was performed under isoflurane anesthesia administered with a vaporizer (5% for induction and 2.5% for maintenance during surgery). Buprenorphine (75 μg/kg body wt) was administered subcutaneously for perioperative pain relief. After a 2-wk recovery period, NPX animals were divided into two groups and treated or not with 1% NaCl in drinking water and 75 mg/kg body wt DOCA dissolved in sunflower oil and administered subcutaneously 3 times/wk for 6 wk (35) [NPX/DOCA/NaCl (NDS) group]. Untreated animals were injected three times weekly with vehicle. Animals from the four experimental groups were housed in metabolic

cages. After a 2-day adaptation period, samples were collected for 2 consecutive days. Food and water intake as well as urinary and fecal output were measured daily. Urine samples were centrifuged for 10 min at 13,000 *g* and stored at −80°C for further analysis. Urinary Na^+, K^+, and Cl^- content was measured using ion-selective electrodes (Cobas c501, Roche Diagnostics). Urinary creatinine and albumin concentrations were measured using commercially available kits (Creatinine Assay Kit and Mouse Albumin ELISA, Abcam). Systolic blood pressure (SBP) was measured by tail-cuff plethysmography in trained conscious mice using a noninvasive blood pressure measuring system for rodents (model LE5007, Harvard Apparatus Panlab). Data were acquired with SeDaCom 2.0 software. Measurements were collected for 3 consecutive days after 5 days of training. SBP was measured at 20-min intervals for 1 h between 10 and 11 AM. GFR measurements used a simplified method of iohexol plasma clearance that we have previously validated in mice (36). Briefly, a single dose of iohexol (6,47 mg Omnipaque 300, GE Healthcare) was injected intravenously into the tail vein in mice lightly sedated with isoflurane (2.5%), administered by facemask whereas the tail vein was dilated using a heating blanket. Blood samples (≤10 μL) were collected at 15, 35, 55, and 75 min after injection from a small cut in the tail using a heparinized capillary tube. Plasma iohexol concentrations were measured by HPLC. Internal calibration curves of iohexol were prepared for each set of samples. Plasma concentrations (C_{plasma}) of iohexol were recalculated from blood levels (C_{blood}) using the following formula: $C_{plasma} = C_{blood}/1 - Hct$, where Hct is the hematocrit. Measured iohexol concentrations were fitted by a slope-intercept method according to a one-compartment model simplified method (36). Fractional excretion of Na^+ (FE_{Na+}) was expressed as the percentage of the filtered Na^+ load (calculated from plasma Na^+ concentration and GFR) excreted in the urine (37). After treatments, mice were euthanized by carbon dioxide inhalation followed by cervical dislocation.

Tissue Sampling, Plasma Measurements, Histological Analysis, and Cell Culture

After euthanasia, blood was collected by cardiac puncture. Serum corticosterone and aldosterone levels were determined with commercial ELISA kits (DRG Diagnostics). Plasma Na^+, K^+, and Cl^- concentrations were measured using ion-selective electrodes (Cobas c501, Roche Diagnostics). Tissues were collected from control and treatment groups at the same time and under the same conditions and processed and analyzed in parallel. Kidneys were removed, weighed, frozen in liquid nitrogen, and stored at −80°C for molecular analysis or fixed by immersion in 4% formaldehyde, paraffin embedded, and processed for histology. Kidney 3-μm-thick microtome sections were stained with 0.1% sirius red in saturated picric acid. Sections were codified to conduct a blinded quantification of fibrosis area. To that end, images from five different fields in each section were collected at ×40 magnification, and the fibrotic area was quantified using Fiji software (ImageJ, National Institutes of Health) (38). Two independent experiments were analyzed (first experiment, $n = 7$ animals in each group; second experiment, $n = 5$ animals in each group). Primary mouse embryonic fibroblasts (MEFs) were derived from wild-type (WT) and Tg.sgk1 embryos and cultured as previously described (39). The kidney slice preparation was performed as previously described (40). Briefly, kidneys from untreated WT or Tg.sgk1 animals were collected in ice-cold Ringers-type buffer [containing (in mM) 98.5 NaCl, 35 $NaHCO_3$, 3 KCl, 1 NaH_2PO_4, 2.5 $CaCl_2$, 1.8 $MgCl_2$, and 25 glucose] and sectioned with a vibration microtome (Microm HM650, Thermo Scientific) to obtain 280-μm-thick slices. Tissue slices were then transferred to Ringers-type buffer modified to contain 25 mM $NaHCO_3$ and incubated for 2 h at 25°C while being constantly bubbled with carbogen (95% O_2-5% CO_2). When indicated, incubation included 50 μM of the SGK1-specific inhibitor EMD638683 (1). Control slices included the same amount of vehicle (DMSO, 1:1000 dilution). After 2 h, slices were transferred to lysis buffer [0.5 M Tris base (pH 7.4), 10% SDS, and phosphatase and proteinase inhibitors] and processed for Western blot analysis as described below.

Microarray Analysis and Quantitative RT-PCR

Total RNA was obtained from tissues disrupted with a Tissue Tearor (BioSpec Products) or from cultured cells using a commercial kit (Total RNA Spin Plus, REAL, Valencia, Spain), which includes an in-column treatment with DNase I. Purified total RNA was quantified using a Nanodrop 1000 (Thermo Scientific). Whole transcriptome analysis was performed using RNA from the kidney cortex of NDS-treated WT and Tg.sgk1 mice ($n = 4$ in each group). RNA quality analysis was performed using an Agilent 2100 Bioanalyzer. cDNA was synthesized using the GeneChip WT PLUS Reagent Kit (Affymetrix) and analyzed by hybridization to a GeneChip Mouse Gene 2.0 ST Array (Affymetrix). MIAME-compliant microarray data have been deposited in the Gene Expression Omnibus (GEO) repository (National Center for Biotechnology Information, National Institutes of Health) under Accession Number GSE148880. Raw files were normalized with rma using oligo package in R (41), whereas differential expression analysis was performed using the limma package (42). A cutoff level of 0.15 (false discover rate) was used for obtaining the volcano plot (https://github.com/kevinblighe/EnhancedVolcano) and STRING protein-protein interaction network (43), which were visualized in Cytoscape (44). Gene Ontology (GO) (45) enrichment analysis was performed with a false discovery rate = 0.3 cutoff using the clusterProfiler package in R (46). Relative mRNA abundance was examined by quantitative RT-PCR (qPCR). Equal amounts of total RNA were processed with the iScript cDNA synthesis kit (Bio-Rad). Gene expression was assessed using commercially available Taqman primer/probe sets (ThermoFischer) or specific oligonucleotide pairs (Table 1) and SYBR Green supermix (Bio-Rad).Relative expression of the target genes was calculated with the comparative threshold cycle method (47) using GAPDH as the normalizer. Housekeeper expression stability was analyzed using qbase+ software (Biogazelle) (48).

Western Blot Analysis

Protein extracts from frozen tissue or kidney slices were quantified using the bicinchoninic acid procedure. Equal amounts of protein were resolved on SDS-PAGE (10% Mini-PROTEAN TGX Stain-Free Gels, Bio-Rad) and transferred to polyvinyl difluoride membranes (Bio-Rad). Western blots were

Table 1. *Primers and quantitative RT-PCR probe sets used in this study*

Gene	Forward	Reverse	Use
Gapdh	5′-ATGGGAAGCTGGTCATCAAC-3′	5′-GTGGTTCACACCCATCACAA-3′	qPCR
Sgk1	5′-GGAAGCAGCAGAAGCCTTCCTCGG-3′	5′-GACTGCCAAGCTTCCGGTGTGC-3′	RT-PCR
Sgk1	5′-CGGTTTCACTGCTCCCCTCAG-3′	5′-GCGATGAGAATCGCTACCATT-3′	qPCR
Ctgf	5′-CTGCCTACCGACTGGAAGACACATT-3′	5′-TCTCCAGTCTGCAGAAGGTATTGTC-3′	qPCR
Col1a1	5′-TGCCGTGACCTCAAGATGTG-3′	5′-CACAAGCGTGCTGTAGGTGA-3′	qPCR
Col4a1	5′-CAAGCATAGTGGTCCGAGTC-3′	5′-AGGCAGGTCAAGTTCTAGCG-3′	qPCR
Fn1	5′-ACGATGGAAGACCTACGGATGTA-3′	5′-TCAGCTTGCACATCTAACGGCAT-3′	qPCR
Acta2	5′-TGCTATGTCGCTCTGGACTTTGA-3′	5′-ATGAAAGATGGCTGGAAGAGG GTC-3′	qPCR
Kim-1	5′-ATGAATCAGATTCAAGTCTTC-3′	5′-TCTGGTTTGTGAGTCCATGTG-3′	qPCR
Lcn2	5′-GGACCAGGGCTGTCGCTACT-3′	5′-GGTGGCCACTTGCACATTGT-3′	qPCR
Ccl2	5′-GTCACCAAGCTCAAGAGAGA-3′	5′-GTGGAAAAGGTAGTGGATGC-3′	qPCR
	Probe set		
Gapdh	TaqMan Mm99999915_g1 (ThermoFisher)		qPCR
Tgfb1	TaqMan Mm 01178820_m1 (ThermoFisher)		qPCR
Col27a1	TaqMan Mm01267526_m1 (ThermoFisher)		qPCR
Lyplal1	TaqMan Mm00525055_m1 (ThermoFisher)		qPCR
Cpb2	TaqMan Mm00490698_m1 (ThermoFisher)		qPCR
Serpina3b	TaqMan Mm00557205_m1 (ThermoFisher)		qPCR
Ccl28	TaqMan Mm00445039_m1 (ThermoFisher)		qPCR
Adamtsl2	TaqMan Mm01326794_m1 (ThermoFisher)		qPCR

In the case of the TaqMan probe sets, catalog numbers are indicated. *Acta2*, smooth muscle actin, α_2; *Adamtsl2*, ADAMTS-like 2; *Ccl2*, chemokine (C-C motif) ligand 2 [monocyte chemoattractant protein-1 (MCP-1)]; *Ccl28*, chemokine (C-C motif) ligand 28; *Col1a1*, collagen type I-α_1; *Col4a1*, collagen type IV-α_1; *Col27a1*, collagen type XXVII-α_1; *Cpb2*, carboxypeptidase B2; *Ctgf*, connective tissue growth factor; *Gapdh*, glyceraldehyde-3-phosphate dehydrogenase; *Fn1*, fibronectin 1; *Kim-1*, kidney injury molecule 1 (Havcr1); *Lcn2*, lipocalin-2 [neutrophil gelatinase-associated lipocalin (NGAL)]; *Lyplal1*, lysophospholipase-like 1; *Serpina3b*, serine (or cysteine) peptidase inhibitor, clade A, member 3B; *Tgfb1*, transforming growth factor-β1.

performed as previously described (49). Phosphorylation of GSK-3α/β at residue Ser^{21}/Ser^{9} was analyzed with a phospho-specific antibody (no. 9331, Cell Signaling). Signals were normalized to total expression of GSK-3β, obtained with rabbit monoclonal antibody (no. 9315, Cell Signaling). Total and phosphorylated NEDD4-2 were detected using rabbit antibodies anti-NEDD4-2 (no. 4013S) and anti-phosphorylated (p)NEDD4-2-S448 (no. 8063S, Cell Signaling). Neutrophil gelatinase-associated lipocalin (NGAL) was detected with polyclonal goat antibody (AF1857, R&D Systems). Signals were acquired with a chemiluminescent detector (ChemiDoc Imaging System, Bio-Rad) and quantified using software provided by the manufacturer. Phosphorylation in each individual sample was calculated as the signal intensity obtained with the phospho-specific antibody divided by the signal intensity obtained in the same sample with antibody against the total protein. Each data point was then normalized to the average value in the WT condition. NGAL protein abundance was calculated as the signal intensity of each band divided by the total signal intensity obtained in the same gel by total protein staining using the Stain-Free method (Bio-Rad) (50).

Statistical Analysis

Statistical analysis was performed with Prism 8 software (Graphpad, San Francisco, CA). Tests are indicated in each figure or table.

RESULTS

Transgenic Expression of Constitutively Active SGK1 in the Kidney Increases Phosphorylation of Downstream Targets

Total expression of SGK1 mRNA was analyzed in renal cortex samples of WT and Tg.sgk1 mice. We confirmed the expression of the transgene in kidney by RT-PCR using primers flanking the triple HA tag inserted in the COOH-terminus of Tg.sgk1 (Fig. 1*A*). As we have previously shown in other tissues (31, 32), Tg.sgk1 animals showed two bands corresponding to endogenous SGK1 and the HA-labeled transgenic SGK1, respectively, whereas control animals showed only the lower band corresponding to the endogenous gene (Fig. 1*B*). The abundance of SGK1 transcript in the renal cortex of control and Tg.sgk1 mice was examined by qPCR. Tg.sgk1 mice showed an approximately twofold increased expression of SGK1, consistent with the use of a BAC containing the physiological SGK1 promoter (Fig. 1*C*). Treatment with the mineralocorticoid DOCA in the context of high NaCl intake significantly increased SGK1 expression in transgenic but not WT animals (Fig. 1*C*). This suggests that constitutively active SGK1 may potentiate its own expression under certain conditions and is like what we have previously found in the liver of animals treated with a high-fat diet (21). To check whether transgenic expression of gain-of-function SGK1 mutant produces increased downstream signaling, we tested the phosphorylation of GSK-3α/β at residues Ser^{21}/Ser^{9}, a well-known target of SGK1 (51). Comparison between WT and Tg.sgk1 animals showed an ~50% increase in pGSK-3α/β abundance (Fig. 1, *D* and *E*), in agreement with data obtained from other tissues (21). We further tested SGK1 target phosphorylation in kidney slices incubated for 2 h in Ringers-type solution ex vivo. This approach allowed us to detect more robust changes in target phosphorylation because of constitutive SGK1 activity by minimizing other stimuli present in vivo. In addition to pGSK-3α/β, our analysis included NEDD4-2 phosphorylation at residue Ser^{448}, an important functional target of SGK1 activity in the kidney (8, 9). We detected significantly increased pGSK-3α/β and pNEDD4-2 in kidney tissue from transgenic animals (Fig. 1, *F* and *I*), a difference that was abrogated when slices were incubated with the SGK1-specific inhibitor EMD638683 (Fig. 1, *F–I*).

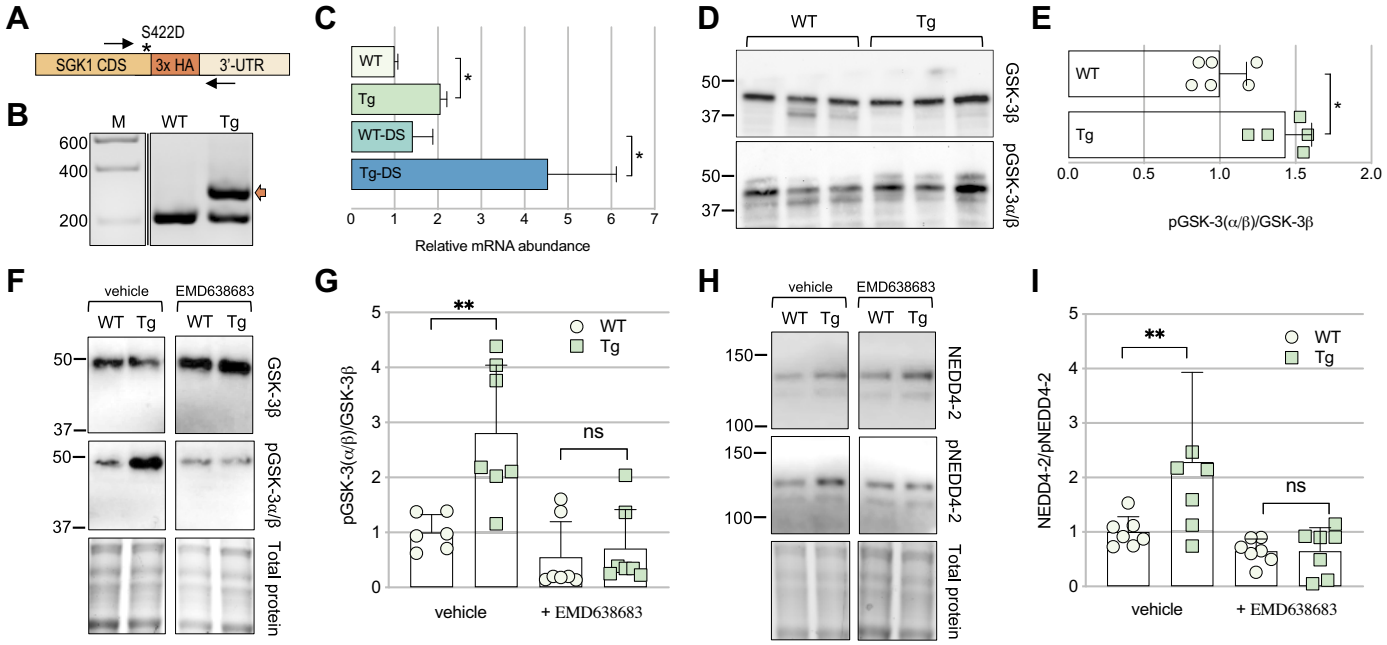

Figure 1. Transgenic (Tg) expression of constitutively active serum and glucocorticoid-regulated kinase 1 (SGK1) in the kidney and increased phosphorylation of the SGK1 downstream target glycogen synthase kinase (GSK)-3. *A*: schematic representation of the 3′-end of the modified *Sgk1* gene, including three copies of the HA tag (3× HA) and point mutation S422D, which renders the kinase constitutively active (*). Arrows indicate oligonucleotides used to simultaneously detect endogenous and transgenic SGK1 by RT-PCR. 3′-UTR, 3′-untranslated region. *B*: agarose gel electrophoresis analysis of RT-PCR products obtained from wild-type (WT) or Tg kidney cortex cDNA using the oligonucleotide pair shown in*A*. M, molecular mass makers (values in bp). Arrow indicates the additional PCR product because of the presence of the transgene. *C*: relative SGK1 mRNA abundance in the indicated WT and Tg.sgk1 mouse experimental groups. DS, mice treated with DOCA/NaCl. Bars represent averages ± SE ($N = 6-8$) normalized to GAPDH expression. One-way ANOVA followed by Tukey's multiple comparison test was used for statistical analysis (*$P < 0.05$). *D*: representative Western blots of kidney lysates from WT and Tg mice were probed with anti-GSK-3β or anti-phospho-GSK-3α/β (pGSK-3α/β) antibodies. Lines indicate molecular mass marker migration (values in kDa). *E*: relative abundance of pGSK-3α/β in WT and Tg.sgk1 kidney lysates. Each point represents signal intensity obtained with anti-pGSK-3α/β divided by the signal intensity obtained in the same sample with anti-GSK-3α/β and normalized to the average value in the WT condition. Bars represent averages ± SD ($n = 6$) of pGSK3β/GSK3β normalized to WT. *$P < 0.05$ (by an unpaired *t* test). *F*: representative Western blots of kidney slice lysates from WT and Tg mice incubated *ex vivo* for 2 h in the presence or absence of the SGK1 inhibitor EMD638683 and probed with anti-GSK-3β or anti-pGSK-3α/β antibodies. Lines indicate molecular mass marker migration (values in kDa). *G*: relative abundance of pGSK-3α/β in kidney slice lysates. Points represent data points from individual animals. Bars represent averages ± SD ($n = 6-7$) of pGSK3β/GSK3β normalized to the WT group under control (vehicle) conditions. ns, Not significant. **$P < 0.01$ (by an unpaired *t* test). *H*: representative Western blots of kidney slice lysates obtained as described in *F* but probed with anti- neural precursor cell expressed developmentally downregulated 4-like (NEDD4-2) or anti-phospho-S448-NEDD4-2 (pNEDD4-2) antibodies. *I*: relative abundance of pNEDD4-2 in kidney slice lysates. Points represent data points from individual animals. Bars represent averages ± SD ($n = 7$) of pNEDD4-2/NEDD4-2 normalized to the WT group. **$P < 0.01$ (by an unpaired *t* test).

NPX and DOCA/NaCl Treatment Increases Blood Pressure to the Same Extent in WT and Tg.sgk1 Mice

Two-kidney untreated Tg.sgk1 mice did not show any change in systemic blood pressure compared with WT animals, even when animals were treated with DOCA/NaCl (Fig. 2). NPX did not alter blood pressure in Tg.sgk1 or WT mice compared to two-kidney animals (Fig. 2). Blood pressure increased after 4 wk DOCA/NaCl treatment of NPX animals (NDS challenge) from both genotypes (Fig. 2). NDS lowered aldosterone circulating levels in WT animals, as expected, but no significant changes were detected in NDS Tg.sgk1 animals compared with NPX (Table 2). There were no differences in water intake, diuresis, and plasma or urine electrolytes between genotypes (Table 2).

Excess SGK1 Activity Exacerbates Albuminuria and Increases Glomerular Filtration After NPX and DOCA/NaCl Treatment

To evaluate the effect of SGK1 on glomerular function during the NDS challenge, we measured urinary albumin excretion and GFR. The basal urinary albumin-to-creatinine ratio was equal in WT and Tg.sgk1 mice and was enhanced by DOCA/NaCl treatment (Fig. 3*A*). Most importantly, the urinary albumin-to-creatinine ratio was significantly higher in Tg.sgk1 mice (Fig. 3*A*), suggesting damage in the glomerular filtration barrier. Iohexol clearance measurements did not reveal any significant difference between untreated WT and Tg.sgk1 mice (Fig. 3*B*), with GFR values consistent with our previously reported results for male mice from the same strain (36). NPX induced a decrease in GFR, as expected, with no significant differences between genotypes (Fig. 3*B*). When NPX animals were treated with DOCA/NaCl, GFR increased significantly only in Tg.sgk1 animals but not in WT animals (Fig. 3*B*). To functionally assess possible tubular injury, we measured FE_{Na+}. FE_{Na+} in NPX mice was undistinguishable between WT and Tg.sgk1 mice (~0.3%; Fig. 3*C*) and within the normal range (37, 52). DOCA/NaCl increased FE_{Na+}, as expected, but no significant difference was detected between WT and transgenic mice (Fig. 3*C*).

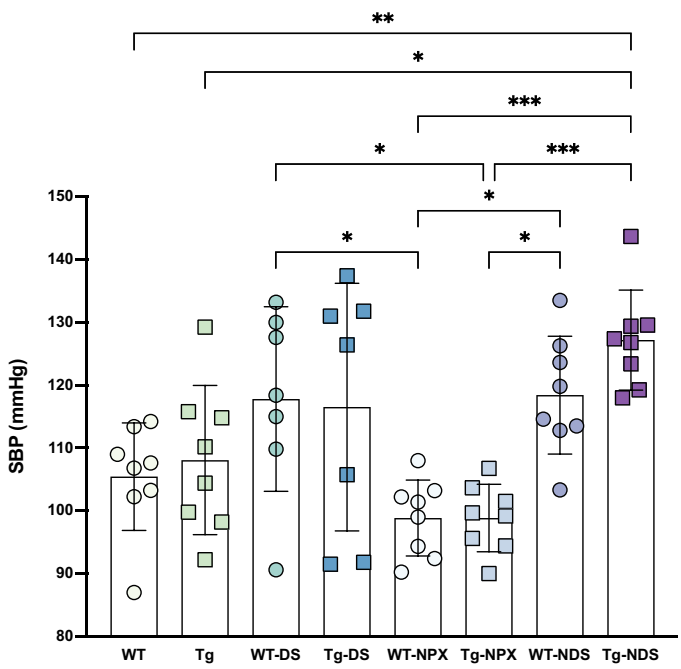

Figure 2. DOCA/NaCl (DS) increases systolic blood pressure (SBP) in unilateral nephrectomized (NPX) mice without significant differences between genotypes. Two-kidney or NPX animals were left untreated or treated with DS for 6 wk. SBP was measured by tail-cuff plethysmography. NDS, NPX animals treated with DS; Tg, transgenic; WT, wild type. Points represent average SBP in individual animals. Bars represent means ± SD ($n = 6 - 8$). Measurements were compared using one-way ANOVA followed by a Tukey's multiple comparison test. *$P < 0.05$; **$P < 0.01$; ***$P < 0.001$. For clarity, nonsignificant differences are not explicitly indicated.

Tg.sgk1 Mice Display Aggravated Glomerular Hypertrophy, Fibrosis, and Inflammation Under NDS Treatment

NDS treatment significantly increased kidney weight in both WT and transgenic animals, without significant differences between genotypes (Table 2). Evaluation of excess SGK1 activity on NDS-induced changes in kidney morphology and fibrosis was analyzed using Sirius red staining (Fig. 4, *A* and *B*). Upon NPX, Tg.sgk1 mice showed glomerular hypertrophy, an effect that was further potentiated when animals were treated with DOCA/NaCl (Fig. 4*A*). Quantification of Sirius red-positive areas in the kidney cortex revealed increased glomerular and interstitial fibrosis, with a tendency toward increased perivascular fibrosis, in Tg.sgk1 mice compared with WT mice after NDS (Fig. 4*C*). We next examined the expression of molecular markers of fibrosis in the kidney cortex. SGK1 has previously been implicated in promoting the expression of connective tissue growth factor (CTGF) (53), a gene involved in the pathogenesis of fibrosis. DOCA/NaCl treatment significantly increased CTGF expression in transgenic animals but not in their WT counterparts. There was no significant induction of transforming growth factor (TGF)-β1 (Fig. 4*D*), consistently with the previously described aldosterone-induced profibrotic pathway mediated by CTGF through a TGF-β1-independent pathway. Fibronectin and collagen type IV were significantly upregulated after DOCA/NaCl in both Tg.sgk1 and WT mice, whereas α-smooth muscle actin did not show any significant change with the treatment (Fig. 4*D*). Surprisingly, collagen type I was less induced in transgenic animals than in WT animals (Fig. 4*D*), in contrast to what could be predicted based on data using SGK1 knockout (54). Expression of monocyte chemoattractant protein-1 [MCP-1; chemokine (C-C motif) ligand (Ccl2)], a marker of inflammation, was significantly upregulated by NDS challenge, although induction was slightly smaller in Tg.sgk1 mice (Fig. 4*D*). Given the increased tubulointerstitial fibrosis in Tg.sgk1 animals, we also asked whether molecular markers of tubular injury such as NGAL (lipocalin 2) and kidney injury molecule-1 (KIM-1) (55) were altered in transgenic mice. We detected no changes in KIM-1 expression and small but significantly increased NGAL expression in DOCA/NaCl-treated transgenic animals (Fig. 4*D*). Based on this result, we decided to explore further NGAL expression and performed Western blot analysis with kidney cortex lysates taken from the four experimental groups. Our results did not reveal any significant change in NGAL protein expression (Fig. 4, *E* and *F*). These results, together with unaffected FE_{Na+} (Fig. 3*C*), suggest the absence of significant tubular injury in this model.

Differentially Regulated Genes in Tg.sgk1 Animals in Response to DOCA/NaCl

To identify potential genes involved in the aggravated kidney injury observed in Tg.sgk1 animals following NDS, we

Table 2. *General characteristics of WT and Tg.sgk1 mice subjected to NPX and treated or not with NDS*

Variable	NPX		NDS	
	WT	Tg.sgk1	WT	Tg.sgk1
Kidney weight†	8.0 ± 0.7 ($n = 10$)	8.0 ± 0.4 (n = 10)	10.3 ± 0.8 (n = 12)*	10.5 ± 1.0 (n = 10)*
Aldosterone (nM)	1.51 ± 0.59 (n = 4)	1.15 ± 0.21 (n = 4)	0.77 ± 0.36 (n = 5)*	0.66 ± 0.25 (n = 5)
Corticosterone (nM)	110 ± 17 (n = 4)	55 ± 16 (n = 4)	141 ± 52 (n = 5)	85 ± 30 (n = 5)
Plasma Na^+ (mM)	151.5 ± 1.9 (n = 5)	150.0 ± 0.9 (n = 5)	152.0 ± 1.3 (n = 6)	150.8 ± 2.4 (n = 5)
Plasma K^+ (mM)	7.4 ± 0.1 (n = 5)	6.6 ± 0.3 (n = 5)	6.8 ± 0.3 (n = 6)	7.0 ± 0.4; n = 5
Plasma Cl^- (mM)	105.0 ± 1.1 (n = 5)	102.3 ± 0.6 (n = 5)	105.0 ± 0.8 (n = 6)	102.8 ± 1.7 (n = 5)
Urine Na^+ (mM)	71.2 ± 4.4 (n = 5)	74.0 ± 13.3 (n = 5)	273.0 ± 15.7 (n = 6)*	260.0 ± 27.7 (n = 5)*
Urine K^+ (mM)	235.1 ± 17.2 (n = 5)	209.7 ± 30.7 (n = 5)	27.8 ± 5.0 (n = 6)*	33.0 ± 7.5 (n = 5)*
Urine Cl^- (mM)	160.6 ± 17.2 (n = 5)	162.6 ± 26.7 (n = 5)	292.3 ± 17.0 (n = 6)*	276.3 ± 33.3 (n = 5)*
Diuresis (ml/24 h)	1.33 ± 0.22 (n = 5)	1.76 ± 0.46 (n = 5)	5.31 ± 0.22 (n = 6)*	5.74 ± 0.19 (n = 5)*
Water intake (ml/24 h)	5.74 ± 0.51 (n = 5)	8.42 ± 1.34 (n = 5)	11.4 ± 0.56 (n = 6)*	13.5 ± 2.01 (n = 5)*

Results are expressed as averages ± SD (n, number of animals). NDS, unilateral nephrectomy with DOCA/NaCl challenge; NPX, unilateral nephrectomy; Tg.sk1, transgenic serum and glucocorticoid-regulated kinase 1; WT, wild-type. Statistical significance was analyzed using one-way ANOVA followed by a Tukey's multiple comparison test. There were no significant differences between genotypes in NPX or NDS groups. *$P < 0.05$ compared with the same genotype. †normalized to body weight × 1,000.

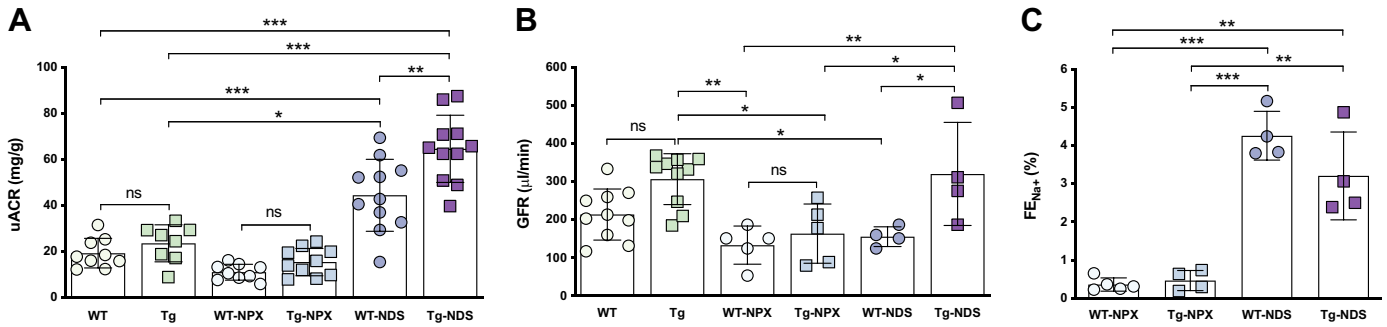

Figure 3. Increased serum and glucocorticoid-regulated kinase 1 (SGK1) activity exacerbates albuminuria after unilateral nephrectomy (NPX) and DOCA/NaCl (DS) challenge. *A*: urinary albumin-to-creatinine ratio (uACR). Data points represent measurements from individual mice. Bars represent experimental group averages ± SD ($n = 8-12$). Measurements were compared using one-way ANOVA followed by a Tukey's multiple comparison test. $^{*}P < 0.05$; $^{**}P < 0.01$; $^{***}P < 0.001$. ns, Not significant. *B*: glomerular filtration rate (GFR) was measured using the iohexol plasma clearance method in control wild-type (WT) or transgenic (Tg) animals ($n = 10$), NPX animals (WT-NPX and Tg-NPX, $n = 5$), and NPX animals after 5 wk of DS treatment (WT-NDS and Tg-NDS; $n = 4$). Bars represent experimental group averages ± SD. Measurements were compared using one-way ANOVA followed by a Tukey's multiple comparison test. $^{*}P < 0.05$; $^{**}P < 0.01$. ns, Not significant. *C*: fractional excretion of Na^+ (FE_{Na+}; in %). Individual points represent values from each animal ($n = 4-5$). Bars represent averages ± SD. Measurements were compared using one-way ANOVA followed by a Tukey's multiple comparison test. $^{**}P < 0.01$; $^{***}P < 0.001$.

performed whole-transcriptome analysis using microarrays. Our analysis compared WT and Tg.sgk1 mice subjected to the challenge ($n = 4$ in each group). Differential expression analysis by limma resulted in the identification of 198 probe sets, of which 120 were upregulated and 78 were downregulated at the given false discovery rate (false discovery rate < 0.15; see Supplemental Table S1, All Supplemental Material is available online at https://doi.org/10.6084/m9.figshare.12973016.v1) based on the volcano plot (Fig. 5*A*). Among these significantly modulated genes, there were more upregulated ($n = 38$) than downregulated ($n = 9$) probe sets exhibiting a $\log_2$ fold change greater than or equal to 1 (red probe sets; Fig. 5*A*). Carboxypeptidase B2 (*Cpb2*) and serpin D1A (*Serpind1a*) were the most significantly modulated upregulated and downregulated genes, respectively (Supplemental Table S1). The hierarchical clustering of expression values of the genes obtained from the differential expression analysis demonstrated that there were two main clusters separating samples from WT and Tg.Sgk1 animals, respectively, as well as two clusters of genes exhibiting upregulation and downregulation of expression (Fig. 5*B*) with relatively stable within-cluster variability. The gene modules obtained for proteins with a physical- and/or context-driven interaction (String Database) between them were drawn by Cytoscape and helped identify the specific gene clusters/modules for the differentially expressed genes. There were two relatively large gene modules with 15 and 8 members each, respectively. The 15-member gene network included the most significantly upregulated gene, *Cpb2*, along with several genes involved in collagen fibril formation, e.g., lysyl oxidase-like (*Loxl*), collagen type I-α_1 (*Col1a1*), and the collagen type XXVII α_1-chain (*Col27a1*; Fig. 5*C*). On the other hand, the 8-member gene network included mostly the serpin A (*Serpina*) gene family in which *Serpina1* and *Serpina3* genes were down- and upregulated, respectively (Fig. 5*C*). Two other smaller networks were also observed; one contained upregulated members of cytoplasmic dynein family (*Dynlt1*) genes, known to be involved in vesicle transport, whereas the other gene module included downregulated genes with relatively less well-known functions in the literature (Fig. 5*C*). Several other 3- or 2-member networks also emerged. We then performed a GO term enrichment analysis using the ClusterProfiler package in R separately for up- and downregulated genes, based on a less stringent false discovery rate cutoff value (i.e., <0.3; see Supplemental Table S2). The resulting pathways for downregulated genes included those involved in extracellular matrix (ECM) formation, whereas upregulated genes belonged to mostly immune response pathways, phagocytosis, as well as lipid metabolism (Fig. 6; see Supplemental Tables S3 and S4).

Among differentially regulated genes detected by microarray analysis, we selected five upregulated genes [*Cpb2*, lysophospholipase-like 1 (*Lyplal1*), *Serpina3b*, chemokine (C-C motif) ligand 28 (*Ccl28*), *and Col27a1*] and one downregulated gene [ADAMTS-like 2 (*Adamtsl2*)] to confirm microarray data by qPCR. Gene selection was based on the following criteria: strong up- or downregulation, statistical significance, and possible relevance to kidney disease based on literature searches. We analyzed a higher number of animals of the same cohort used to perform transcriptomics ($n = 6$) and expanded the analysis to the four groups of animals used throughout this study (NPX WT or Tg.sgk1 with or without DOCA/NaCl treatment). Our results were in accordance to the microarray analysis, showing that the expression of every gene tested was significantly different between WT + NDS and Tg.sgk1 + NDS groups (Fig. 7*A*). Interestingly, when the four experimental groups were examined in parallel, we detected three different patterns of regulation by SGK1 activity and DOCA/NaCl treatment. *Cpb2*, *Ccl28*, and *Serpina3b* were upregulated by increased SGK1 activity, but DOCA/NaCl did not further increase their expression (Fig. 7*A*). This is also the case of *Adamtsl2*, which was downregulated by increased SGK1 activity but unaffected by DOCA/NaCl treatment (Fig. 7*A*). *Lyplal1* was also upregulated by increased SGK1 activity, but DOCA/NaCl additively increased its expression (Fig. 7*A*). In contrast, *Col27A1* was only upregulated by the synergism between increased SGK1 activity and DOCA/NaCl treatment (Fig. 7*A*). We then investigated whether these genes are direct targets of SGK1 signaling or, alternatively, whether their

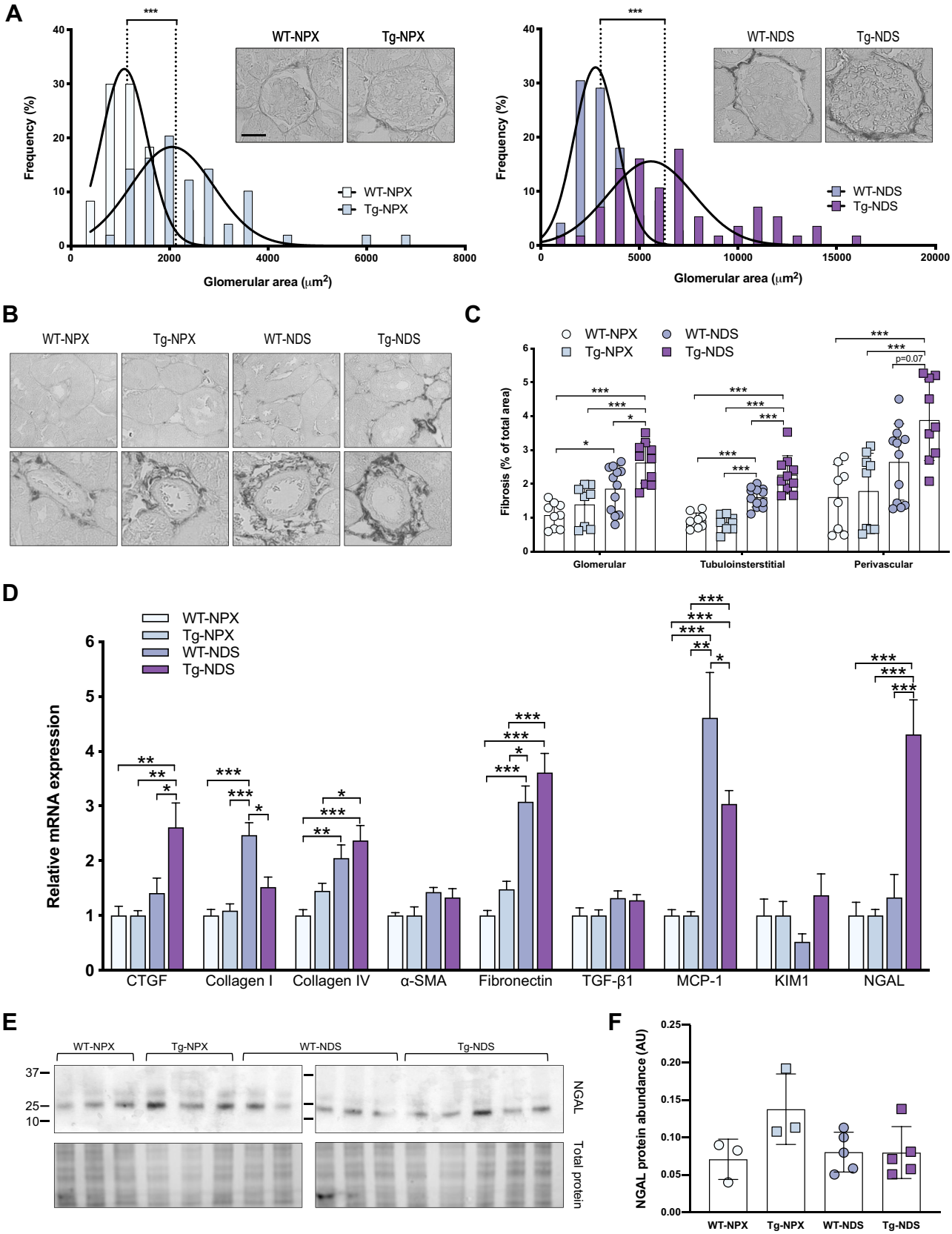

regulation is secondary to the deleterious effects induced by the transgene. To that end, we obtained primary MEFs from WT or transgenic animals (Fig. 7*B*). Of the six genes analyzed, *Col27a1*, *Lyplal1*, and *Ccl28* were detectable in both WT- and Tg.sgk1-derived MEFs (Fig. 7*C*). As expected from the results obtained from kidney samples, *Lyplal1* expression was significantly higher in MEFs derived from Tg.sgk1 mice (Fig. 7*C*). In contrast, *Ccl28* expression was not significantly different between MEFs with the two different genotypes, suggesting that the upregulation detected in vivo may be secondary to other processes triggered by SGK1 in the kidney. *Col27A1* did not show any difference in expression, consistent with the results obtained from animals.

DISCUSSION

This study tested the hypothesis that increased systemic SGK1 activity constitutes a common factor underlying blood pressure-sensitive and -insensitive renal damage secondary to excess mineralocorticoid signaling. To that end, we chose our previously characterized transgenic mouse model with expression of a constitutively active mutant of SGK1 expressed from a BAC (21, 31, 32). This model has the advantage of expressing SGK1 under the control of its own promoter, avoiding overexpression of the kinase but at the same time enhancing downstream signaling. To produce mineralocorticoid-induced increases in blood pressure and development of kidney injury, we used the DOCA/NaCl model, which in mice must be performed in the context of low renal mass (uninephrectomy). Under these conditions, transgenic mice showed significantly increased albuminuria, increased glomerular filtration, glomerular hypertrophy, and fibrosis compared to their WT counterparts, consistent with accelerated kidney damage.

Our results support increased SGK1 activity as a risk factor for the development of mineralocorticoid-dependent kidney injury. In addition, the results shed light on the contribution of the kinase to hypertension-dependent and -independent pathways of renal damage. On one hand, our data showed that SGK1 did not enhance mineralocorticoid-induced increased blood pressure. Previous data have implicated SGK1 in the control of blood pressure in humans and mice. *SGK1* polymorphisms associate with increased blood pressure, hyperinsulinemia (15), and type 2 diabetes (19) in humans. *Sgk1* knockout mice maintain blood pressure at the expense of increased circulating aldosterone, and this strain is unable to maximally activate Na^+ reabsorption after a low Na^+ challenge (11). Lack of *Sgk1* precludes salt-induced hypertension in a high-fat diet context (13) and angiotensin II-induced hypertension (30). Data from our previous studies expanded these observations, showing that enhanced kinase activity exacerbates blood pressure increases in models with a high-fat diet (21). However, in the NDS model used in this work, there was no significant effect of constitutively active SGK1. A longer treatment may be needed to uncover an effect. Alternatively, differences in aldosterone suppression by high salt intake, which was apparent in WT mice but not in Tg.sgk1 mice (Table 2), may mask SGK1 effects on blood pressure. It is important to note that using the same animal model we recently described a significant increase in blood pressure because of a high-fat diet (21), with an average SBP of 170 mmHg after just 7 wk of treatment (40% higher than WT animals). Analysis of these animal cohorts did not show differences in glomerular size or kidney fibrosis (A. Vastola-Mascolo, Velázquez-García, and D. Alvarez de la Rosa, unpublished observations), indicating that during the timeframe used in this and our previously published studies (6–7 wk), increased blood pressure alone is insufficient to produce kidney damage, at least in this genetic background. Also, it should be noted that transgenic NPX animals (not treated with DOCA/NaCl) already demonstrated glomerular hypertrophy (Fig. 4*A*), even though there was no difference in SBP between both genotypes (Fig. 2). Taken together, these results support a role for SGK1 in the early stages of hypertension-independent kidney damage. This is consistent with previously published observations showing that DOCA/NaCl-treated WT and *Sgk1*$^{-/-}$ mice had similar blood pressures but only WT mice developed albuminuria and renal fibrosis (25).

A relevant finding of our study was that renal damage was only observed in the presence of a relevant reduction of renal mass (uninephrectomy). This indicates an interaction between low nephron endowment and SGK1-mediated effects in the induction of renal damage in the context of hypertension. The incidence and prevalence of CKD do not match that of hypertension in humans. Recent studies have indicated that not all subjects with hypertension are at risk for renal disease, only those with concomitant risk factors like metabolic syndrome or low renal mass (56). In fact, a lower number of glomeruli has been associated with a higher risk of hypertension (57). Also, living kidney donors, a healthy population, have an increased risk of hypertension after donation compared with matched healthy controls that

Figure 4. Transgenic (Tg) serum and glucocorticoid-regulated kinase 1 (Tg.sgk1) animals display glomerular hypertrophy and increased fibrosis. *A*: frequency distribution analysis of the glomerular area in the indicated experimental groups. NPX, unilateral nephrectomy; WT, wild-type. *Insets* show representative images of individual glomeruli from 3-μm tissue sections stained with Sirius red. Scale bar = 30 μm. Plot bars represent percentages of glomeruli in each diameter class ($n = 46$). Curves represent Gaussian fitting of the data. Medians of area distribution are indicated by dashed lines. Data were analyzed by a Mann-Whitney test. ***$P < 0.001$. *B*: representative images of the kidney cortex obtained from the indicated experimental groups and stained with Sirius red. *C*: quantification of Sirius red-positive area in glomeruli and interstitial and perivascular regions. Each point represents the average percent positive area obtained from five independent fields for one animal. Bars represent experimental group averages ± SD ($n = 8 - 12$ animals). Data were analyzed by one-way ANOVA followed by a Tukey's multiple comparison test. *$P < 0.05$; ***$P < 0.001$. *D*: relative mRNA levels of the indicated fibrosis and tubular injury markers in WT and Tg.sgk1 mouse experimental groups. α-SMA, α-smooth muscle actin; CTGF, connective tissue growth factor; KIM-1, kidney injury molecule-1; MCP-1, monocyte chemoattractant protein-1; NGAL, Neutrophil gelatinase-associated lipocalin; TGF-β1, transforming growth factor-β1; Bars represent averages ± SD ($n = 5 - 6$) of mRNA abundance values normalized to GAPDH expression. Data were analyzed by one-way ANOVA followed by a Tukey's multiple comparison test. *$P < 0.05$; **$P < 0.01$; ***$P < 0.001$. *E*, *top*: representative Western blots of kidney lysates from WT and Tg mice from the indicated experimental groups and probed with anti-NGAL antibody. Lines indicate molecular mass marker migration (values in kDa). *Bottom*, total protein staining in the same gels using the Stain-Free method (Bio-Rad). *F*: relative NGAL protein abundance. Each point represents signal intensity obtained with anti-NGAL divided by the signal intensity of total protein staining in the same sample. AU, arbitrary units. Bars represent averages ± SD ($n = 3 - 5$) of NGAL/total protein. No significant differences were found using one-way ANOVA followed by Tukey's test.

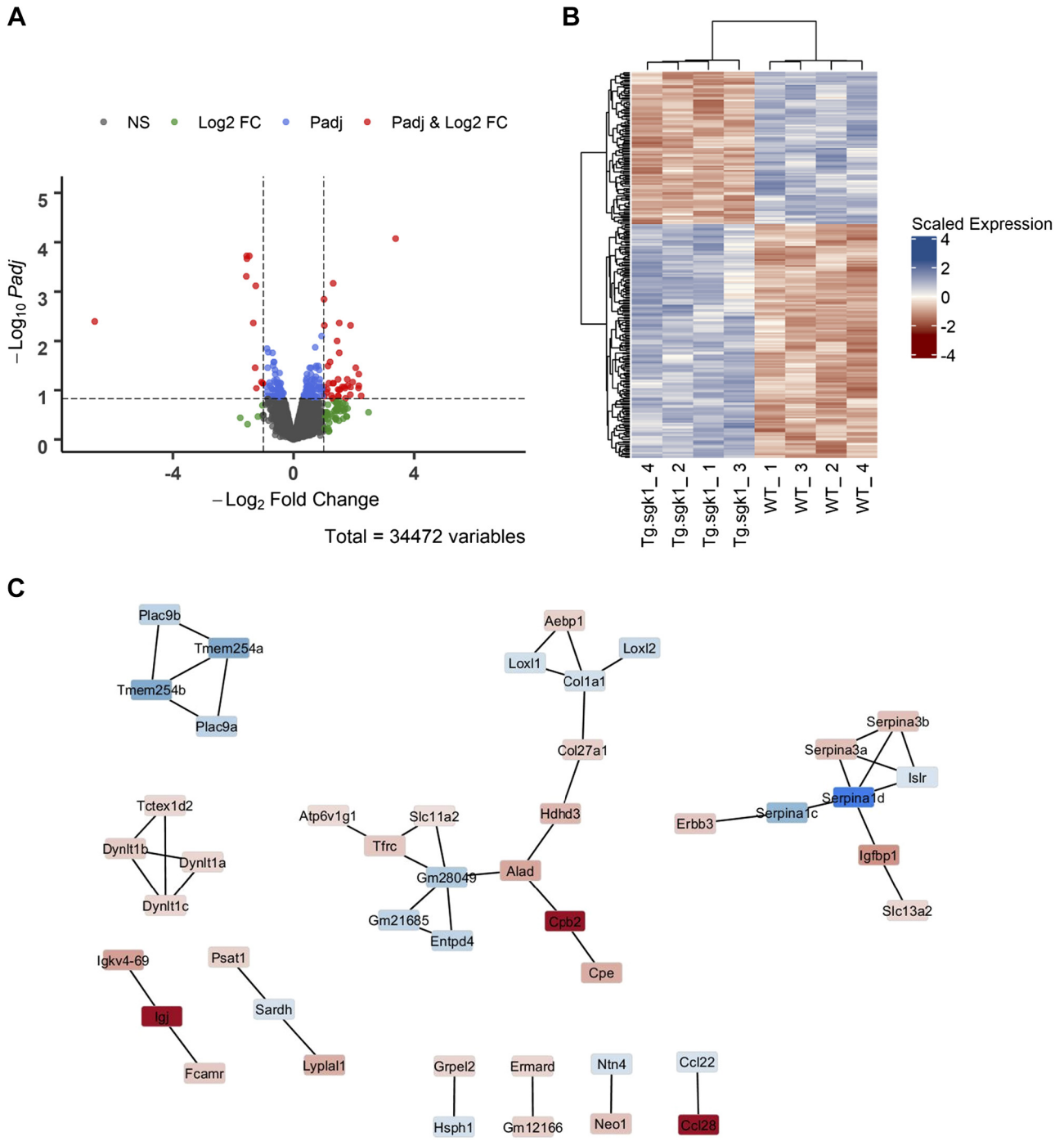

Figure 5. Differentially expressed genes obtained from the microarray experiment. *A*: volcano plot showing the differentially upregulated and downregulated genes along with those not significantly changed. *P* stands for false discovery rate (FDR) < 0.15 whereas the logarithmically (base 2) transformed fold change (log_2FC) is greater than 1 or less than −1. Colors indicate genes that pass the thresholds given by only *P*, only log_2FC, or both. NS, not significant; *P*adj, adjusted *P* value. *B*: heatmap of the differentially expressed genes with an adjusted *P* value threshold of FDR < 0.15. Upregulation and downregulation are represented by the spectrum of red and blue, respectively. *C*: gene network of differentially expressed genes between the groups. Nodes represent genes whose log_2FC values are indicated by colors (pink-blue = up-down, respectively) whereas the edges that connect the nodes refer to the interactions specified by the STRING database. Tg.sgk1, transgenic serum and glucocorticoid-regulated kinase 1; WT, wild-type.

did not undergo NPX (58). These data, together with our results, may support the hypothesis that a reduction of renal mass is necessary to induce hypertension and that SGK1 may play a role in the pathogenesis of renal disease in this context.

The mechanisms involved in the SGK1 contribution to the development of glomerular hypertrophy and glomerular barrier damage are probably diverse. MR-dependent upregulation of SGK1 in podocytes is linked to aldosterone-mediated oxidative stress and glomerular damage (27). In addition,

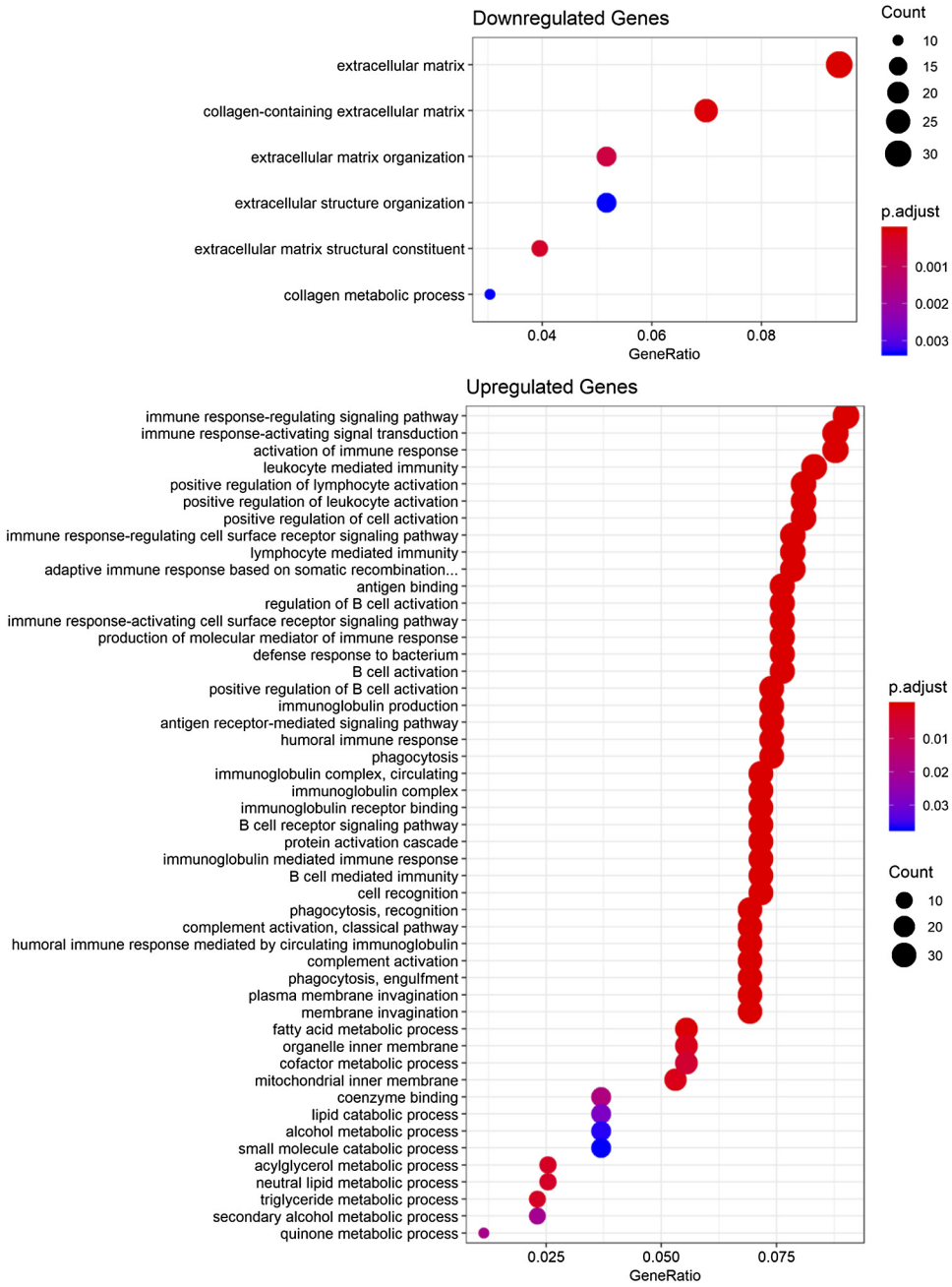

Figure 6. Functional annotation of differentially expressed genes in transgenic serum and glucocorticoid-regulated kinase 1 animals after unilateral nephrectomy with DOCA/NaCl challenge. Gene Ontology (GO) term enrichment analysis for up- and downregulated genes (false discovery rate cutoff value < 0.3) is shown. Adjusted *P* values are indicated using the indicated color scale. Circle diameter is proportional to the number of genes in each GO category.

SGK1 increases ICAM-1 and CTGF expression in mesangial cells, promoting inflammatory and fibrotic responses (59). Our results show increased CTGF expression without changes in TGF-β1 expression in Tg.sgk1 animals, which is consistent with changes reported in aldosterone-induced fibrosis in a rat model of diabetic nephropathy (60). Our results are also in agreement with the lack of TGF-β1 induction in the hearts of DOCA/NaCl-treated mice (53) or rats (61) and the fact that CTGF can be induced independently of TGF-β1 in human mesangial cells (62). In addition, *Sgk1* transcription is upregulated by TGF-β1 (63), and therefore constitutive activation of the kinase appears to control downstream pro-fibrotic pathways. An additional convergence point between SGK1 and TGF-β signaling is provided by NEDD4-L, a ubiquitin ligase that modifies and targets for degradation Smad2/3, mediators of the canonical TGF-β-regulated transcriptional response. SGK1 phosphorylates NEDD4-L, preventing its interaction with Smad2/3 and therefore potentiating TGF-β signaling (64).

We can also speculate about additional pathways that may contribute to the harmful renal SGK1 effects. For instance, insulin-like growth factor-1 (IGF-1), which has been implicated in glomerular hypertrophy in the remnant kidney of the NPX model (65), activates the phosphatidylinositol 3-kinase pathway, and SGK1 is one of the mediators of this pathway. Enhanced activity of MR in additional cell types, such as inflammatory cells, smooth muscle cells, or the endothelium, may cause damage to kidney structure and function.

We have already mentioned that SGK1 expression on antigen-presenting cells contributes to renal inflammation (28). In contrast, endothelial MR knockout prevents cardiac but not renal damage induced by DOCA/NaCl (66). Therefore, SGK1-mediated effects detected in our study are likely independent of endothelial cell function.

To better understand the basic mechanism involved in SGK1-mediated kidney damage, we compared whole transcriptome profiles of the kidney cortex in WT and Tg.sgk1 mice in the NDS model. We detected 120 upregulated and 78 downregulated genes in transgenic mice (false discovery rate < 0.15). To validate microarray results and assess whether our strategy was able to identify genes potentially involved in the exacerbation of DOCA/NaCl kidney injury, we further studied five upregulated genes and one downregulated gene in an independent cohort of animals including the four experimental groups used throughout this study (NPX WT or Tg.sgk1 animals with or without DOCA/NaCl treatment). In every gene tested, we were able to confirm the microarray analysis. Furthermore, we detected different regulation patterns by SGK1 and DOCA/NaCl treatment. Interestingly, *Col27a1* expression was not significantly affected by increased SGK1 activity in the kidney cortex or in cultured primary MEFs. However, the combination of increased SGK1 activity and DOCA/NaCl treatment produced a synergistic increase in *Col27a1*. *Col27a1*, a little-known fibrillar collagen gene that plays a role during the calcification of cartilage and the transition of cartilage to bone (67, 68), has not been previously linked to kidney fibrosis. This result is highly significant, because it validates our strategy to identify genes potentially involved in the amplification of DOCA/NaCl kidney injury by SGK1 activity.

Analysis of gene modules formed by differentially expressed genes uncovered one cluster related to collagen fibril formation (including *Col27a1*, *Col1a1*, and *Loxl*) and the fibrinolytic system (including *Cpb2*), which has also been implicated in the regulation of renal fibrosis (69). GO term enrichment analysis showed an overall downregulation of genes involved in ECM formation. Although this last result may seem paradoxical, taken together the analysis strongly suggests that increased SGK1 leads to dysregulation of pathways controlling ECM remodeling (70). This idea is supported by our analysis of classical fibrosis markers showing the expected overexpression of CTGF, fibronectin, and collagen type IV in Tg.sgk1 mice but not significant changes in TGF-β1 or α-SMA, suggesting alternative pathways for fibrosis development (60). Also, in agreement with this view are previous reports in the literature showing several downregulated ECM components associated with the development of fibrosis. For instance, decorin, one of the downregulated genes in our gene list, is antifibrotic, and decorin knockout mice show increased ECM accumulation in diabetic nephropathy (71). Decorin sequesters TGF-β (72), and, therefore, its downregulation may enhance signaling through

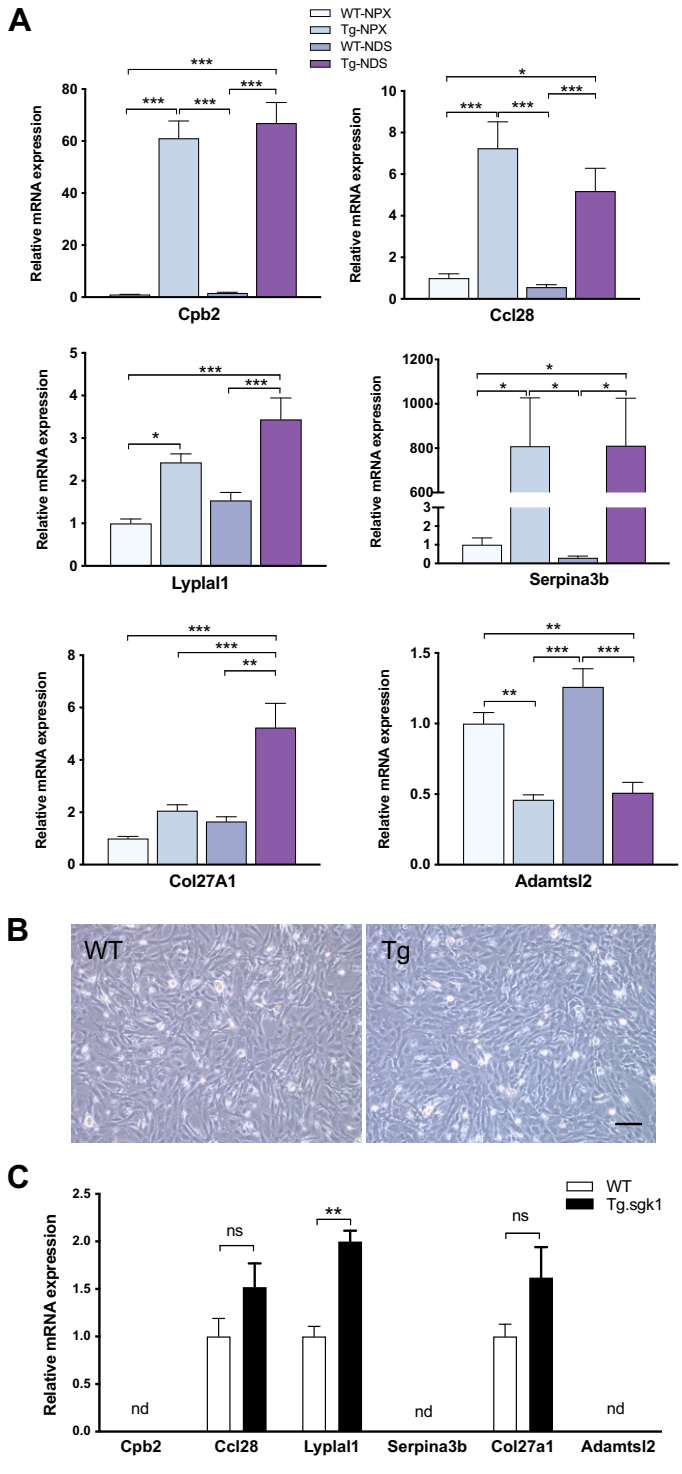

Figure 7. Validation of transcripts predicted by microarray analysis to be differentially regulated in wild-type (WT) or transgenic (Tg) serum and glucocorticoid-regulated kinase 1 (Tg.sgk1) mice after unilateral nephrectomy (NPX) with DOCA/NaCl challenge (NDS). *A*: expression of the indicated genes was assessed by quantitative real-time PCR in the four groups used in this study (WT-NPX, Tg-NPX, WT-NDS, and Tg-NDS). Adamtsl2, ADAMTS-like 2; Ccl2, chemokine (C-C motif) ligand 2; Col, collagen; Cpb2, carboxypeptidase B2; Lyplal1, lysophospholipase-like 1; Serpina3b, serpin A3B. Bars represent averages ± SE ($n = 6$). Statistical analysis was performed by one-way ANOVA followed by Tukey's multiple comparison test. $^*P < 0.05$; $^{**}P < 0.01$; $^{***}P < 0.001$. *B*: representative micrographs of cultured mouse embryonic fibroblasts obtained from WT or Tg.sgk1 embryos. Scale bar = 200 μm. *C*: expression of newly identified differentially expressed genes in mouse embryonic fibroblasts from WT or Tg animals. Bars represent averages ± SE ($n = 6$). Transcripts below the quantitative PCR detection level are indicated by "nd" (not detected). Statistical analysis was performed by one-way ANOVA followed by a Tukey's multiple comparison test. $^{**}P < 0.01$. ns, Not significant difference.

this pathway without alterations in TGF-β mRNA expression. Two membrane-bound matrix metalloproteinases (MMPs; MMP-14 and MMP-15) also come up among the downregulated genes. There is strong evidence pointing to dysregulation of MMPs in a wide variety of kidney diseases, including acute kidney injury, diabetic nephropathy, and glomerulonephritis (73). MMP-14 cleaves several ECM proteins, including collagen type I, fibronectin, and laminin (74). Therefore, MMP-14 has a degradative rather than synthetic role, and its deficiency leads to fibrosis without altering collagen synthesis (75, 76). In addition, both MMP-14 and MMP-15 activate the gelatinase MMP-2, which, together with MMP-9, has extensive implications in kidney disease (74).

Some genes previously characterized as profibrotic showed lower expression in Tg.sgk1 mice compared with WT mice. For instance, *Loxl1*, a member of the lysyl oxidase-like family, cross-links collagen and elastin and has been implicated in fibrogenesis (77). Similarly, upregulation of *Loxl2* may lead to kidney fibrosis in collagen type IV-α_3 (*Col4a3*)-null mice (78). On the other hand, there are reports showing that downregulation of *Loxl2* may increase collagen formation via activation of the TGF-β/Smad pathway in the preeclamptic placenta (79). This suggests that tissue specificity as well as genetic background may determine the effects of ECM regulators such as *Loxl2*. Fibulin-5 (*Fbln5*) (80) and serpin H1 (*Serpinh1*) (81) expression has been linked to the development of kidney fibrosis as well. In addition to the hypothesis that these differentially expressed genes are further indication of dysregulated ECM turnover, it is conceivable that some of them may reflect negative feedback loops limiting the extent of fibrosis development. It is likely that both hypotheses are correct, depending on which individual gene or signaling pathway is being considered.

As mentioned above, the largest gene cluster obtained in our analysis included genes related not only to collagen fibril formation but also to the fibrinolytic system, which participates in the development of renal fibrosis (69). Mice deficient in *Cpb2* [also known as thrombin-activated fibrinolysis inhibitor (TAFI)], the most upregulated gene in the microarray, have better survival and less kidney injury in a sepsis model (82). *Cpb2*/TAFI polymorphisms associate with CKD frequency in a human population (83), whereas its level shows a strong correlation with kidney function impairment. In addition, CPB2/TAFI inhibition ameliorates kidney fibrosis in an animal model of CKD (69). Therefore, our results support a role for the fibrinolytic axis in exacerbated fibrosis observed in Tg.sgk1 mice.

The second largest cluster obtained by gene module analysis includes several members of the serine protease inhibitor clade A (*Serpina*) family. *Serpina1* [α-1-antitrypsin (AAT)], the most downregulated gene in the microarray, has been shown to be the most abundant serine protease inhibitor with prominent anti-inflammatory and tissue-protective effects. *Serpin1a* knockout mice develop lung emphysema (84) and liver fibrosis (85). In addition, AAT therapy protects against kidney injury secondary to ischemia-reperfusion (86). On the other hand, serpina3, a well-known MR target (87) recently proposed as a renal fibrosis and inflammation marker during the transition to CKD (88), is potently upregulated in Tg.sgk1 mice. Accordingly, our findings implicate abnormal accumulation and turnover of a network of ECM proteins in SGK1-driven fibrosis in early-stage CKD.

GO enrichment analysis for upregulated genes uncovered mostly immune response pathways, phagocytosis, and lipid metabolism. Modulation of the immune response and phagocytosis pathways is in good agreement with the well-established role of SGK1 in salt-sensitive hypertension and renal injury through its expression in T cells and antigen-presenting cells (23, 28–30). In fact, T cell-specific and dendritic cell-specific *Sgk1* knockout abrogates increased blood pressure and vascular and renal inflammation in response to DOCA/NaCl treatment (30) and the *N*-nitro-L-arginine methyl ester high-salt protocol (28), respectively. *Ccl28*, a prominently upregulated gene in Tg.sgk1 animals, has previously been characterized as lymphocyte homing factor in mucosal tissues (89) and was recently associated with the accumulation of B and T lymphocytes in the kidney during the transition from acute to chronic injury (90). In addition, the list of differentially expressed genes includes several upregulated genes coding for Ig chains. Taken together, our data not only supports the notion that SGK1 is a key component of T cell infiltration and inflammation in salt-sensitive kidney injury but also supports a role for B cell infiltration in the process (91).

It is important to acknowledge several limitations in our study. First, for practical reasons, we performed experiments on male mice only. However, based on the known sexual dimorphism in blood pressure-dependent and -independent responses in mice (92, 93), additional experiments are needed to assess the role of SGK1 activity on female mice. Also, SGK1 effects on the DOCA/NaCl model are predictably the result of a synergy between pathways regulating renal ion transport, podocyte and mesangial cell function, ECM turnover, and inflammatory responses. Dissecting the role of excess SGK1 activity in each of these components will require using tissue-specific, conditional SGK1 gain-of-function models.

In summary, our results support the idea that systemically increased SGK1 activity is a risk factor for the development of mineralocorticoid-dependent kidney damage, particularly in the context of low renal mass, potentially accelerating the progression to CKD. SGK1 activity alters pathways related to ECM turnover and immune system responses and may provide a therapeutic target to delay CKD development.

SUPPLEMENTAL MATERIAL

Supplemental Tables S1, S2, S3, and S4 can be found at https://doi.org/10.6084/m9.figshare.12973016.v1.

ACKNOWLEDGEMENTS

The authors thank Dr. Frederic Jaisser and Dr. Pablo Martín-Vasallo for critical reading of the manuscript, Dr. Natalia Lopez-Andres and Dr. Eduardo Salido for expert advice on assessing kidney fibrosis, and Dr. Penton Rivas for advice on kidney slice preparation.

GRANTS

This work was funded by Grant BFU2016-78374-R from the Ministerio de Ciencia, Universidades e Innovación (MICINN, Spain) and European Union FP7 COST ADMIRE Network (BM1301). S.V.-G. is supported by Programa Agustin de Betancourt (Cabildo de

Tenerife, Spain). E.P. is a researcher of the Ramón y Cajal Program (MICINN, RYC-2014–16573) and the Red de Investigación Renal (REDinREN, Spain, RD16/0009/0031).

DISCLOSURES

No conflicts of interest, financial or otherwise, are declared by the author(s).

AUTHOR CONTRIBUTIONS

C.S., J.F.N., and D.A. conceived and designed research; C.S., S.V., A.V., A.R., S.L. and G.H. performed experiments; C.S., S.V., A.G.K., A.V., A.R., S.L., G.H., J.F.N. E.P., O.K., and D.A. analyzed data; C.S., S.V., A.G.K., A.V., E.P., O.K., and D.A. interpreted results of experiments; C.S., S.V., A.G.K., and D.A. prepared figures; C.S., O.K., and D.A. drafted manuscript; C.S., S.V., A.G.K., A.V., G.H., J.F.N., E.P., O.K., and D.A. edited and revised manuscript; C.S., S.V., A.G.K., A.V., A.R., S.L., G.H., J.F.N., E.P., O.K., and D.A. approved final version of manuscript.

REFERENCES

1. **Bertocchio JP**, **Warnock DG**, **Jaisser F.** Mineralocorticoid receptor activation and blockade: an emerging paradigm in chronic kidney disease. *Kidney Int* 79: 1051–1060, 2011. doi:10.1038/ki.2011.48.
2. **Rossi GP**, **Bernini G**, **Desideri G**, **Fabris B**, **Ferri C**, **Giacchetti G**, **Letizia C**, **Maccario M**, **Mannelli M**, **Matterello M-J**, **Montemurro D**, **Palumbo G**, **Rizzoni D**, **Rossi E**, **Pessina AC**, **Mantero F.** Renal Damage in Primary Aldosteronism. *Hypertension* 48: 232–238, 2006. doi:10.1161/01.HYP.0000230444.01215.6a.
3. **Barrera-Chimal J**, **Girerd S**, **Jaisser F.** Mineralocorticoid receptor antagonists and kidney diseases: pathophysiological basis. *Kidney Int* 96: 302–319, 2019. doi:10.1016/j.kint.2019.02.030.
4. **Shibata S**, **Fujita T.** Mineralocorticoid receptors in the pathophysiology of chronic kidney diseases and the metabolic syndrome. *Mol Cell Endocrinol* 350: 273–280, 2012. doi:10.1016/j.mce.2011.07.018.
5. **García-Martínez JM**, **Alessi DR.** mTOR complex 2 (mTORC2) controls hydrophobic motif phosphorylation and activation of serum- and glucocorticoid-induced protein kinase 1 (SGK1). *Biochem J* 416: 375–385, 2008. doi:10.1042/BJ20081668.
6. **Ivy JR**, **Jones NK**, **Costello HM**, **Mansley MK**, **Peltz TS**, **Flatman PW**, **Bailey MA.** Glucocorticoid receptor activation stimulates the sodium-chloride cotransporter and influences the diurnal rhythm of its phosphorylation. *Am J Physiol Renal Physiol* 317: F1536–F1548, 2019. doi:10.1152/ajprenal.00372.2019.
7. **Valinsky WC**, **Touyz RM**, **Shrier A.** Aldosterone, SGK1, and ion channels in the kidney. *Clin Sci (Lond)* 132: 173–183, 2018. doi:10.1042/CS20171525.
8. **Debonneville C**, **Flores SY**, **Kamynina E**, **Plant PJ**, **Tauxe C**, **Thomas MA**, **Münster C**, **Chraïbi A**, **Pratt JH**, **Horisberger JD**, **Pearce D**, **Loffing J**, **Staub O.** Phosphorylation of Nedd4-2 by Sgk1 regulates epithelial Na(+) channel cell surface expression. *EMBO J* 20: 7052–7059, 2001. doi:10.1093/emboj/20.24.7052.
9. **Ferdaus MZ**, **Mukherjee A**, **Nelson JW**, **Blatt PJ**, **Miller LN**, **Terker AS**, **Staub O**, **Lin DH**, **McCormick JA.** Mg^{2+} restriction downregulates NCC through NEDD4-2 and prevents its activation by hypokalemia. *Am J Physiol Renal Physiol* 317: F825–F838, 2019. doi:10.1152/ajprenal.00216.2019.
10. **Faresse N**, **Lagnaz D**, **Debonneville A**, **Ismailji A**, **Maillard M**, **Fejes-Toth G**, **Náray-Fejes-Tóth A**, **Staub O.** Inducible kidney-specific Sgk1 knockout mice show a salt-losing phenotype. *Am J Physiol Renal Physiol* 302: F977–985, 2012. doi:10.1152/ajprenal.00535.2011.
11. **Wulff P**, **Vallon V**, **Huang DY**, **Völkl H**, **Yu F**, **Richter K**, **Jansen M**, **Schlünz M**, **Klingel K**, **Loffing J**, **Kauselmann G**, **Bösl MR**, **Lang F**, **Kuhl D.** Impaired renal Na(+) retention in the sgk1-knockout mouse. *J Clin Invest* 110: 1263–1268, 2002. doi:10.1172/JCI15696.
12. **Al-Qusairi L**, **Basquin D**, **Roy A**, **Stifanelli M**, **Rajaram RD**, **Debonneville A**, **Nita I**, **Maillard M**, **Loffing J**, **Subramanya AR**, **Staub O.** Renal tubular SGK1 deficiency causes impaired K+ excretion via loss of regulation of NEDD4-2/WNK1 and ENaC. *Am J Physiol Renal Physiol* 311: F330–342, 2016. doi:10.1152/ajprenal.00002.2016.
13. **Huang DY**, **Boini KM**, **Osswald H**, **Friedrich B**, **Artunc F**, **Ullrich S**, **Rajamanickam J**, **Palmada M**, **Wulff P**, **Kuhl D**, **Vallon V**, **Lang F.** Resistance of mice lacking the serum- and glucocorticoid-inducible kinase SGK1 against salt-sensitive hypertension induced by a high-fat diet. *Am J Physiol Renal Physiol* 291: F1264–1273, 2006. doi:10.1152/ajprenal.00299.2005.
14. **Busjahn A**, **Aydin A**, **Uhlmann R**, **Krasko C**, **Bähring S**, **Szelestei T**, **Feng Y**, **Dahm S**, **Sharma AM**, **Luft FC**, **Lang F.** Serum- and glucocorticoid-regulated kinase (SGK1) gene and blood pressure. *Hypertension* 40: 256–260, 2002. doi:10.1161/01.HYP.0000030153.19366.26.
15. **von Wowern F**, **Berglund G**, **Carlson J**, **Månsson H**, **Hedblad B**, **Melander O.** Genetic variance of SGK-1 is associated with blood pressure, blood pressure change over time and strength of the insulin-diastolic blood pressure relationship. *Kidney Int* 68: 2164–2172, 2005. doi:10.1111/j.1523-1755.2005.00672.x.
16. **Li C**, **Yang X**, **He J**, **Hixson JE**, **Gu D**, **Rao DC**, **Shimmin LC**, **Huang J**, **Gu CC**, **Chen J**, **Li J**, **Kelly TN.** A gene-based analysis of variants in the serum/glucocorticoid regulated kinase (SGK) genes with blood pressure responses to sodium intake: the GenSalt Study. *PLoS One* 9: e98432, 2014. doi:10.1371/journal.pone.0098432.
17. **Rao AD**, **Sun B**, **Saxena A**, **Hopkins PN**, **Jeunemaitre X**, **Brown NJ**, **Adler GK**, **Williams JS.** Polymorphisms in the serum- and glucocorticoid-inducible kinase 1 gene are associated with blood pressure and renin response to dietary salt intake. *J Hum Hypertens* 27: 176–180, 2013.
18. **Friedrich B**, **Weyrich P**, **Stancakova A**, **Wang J**, **Kuusisto J**, **Laakso M**, **Sesti G**, **Succurro E**, **Smith U**, **Hansen T**, **Pedersen O**, **Machicao F**, **Schafer S**, **Lang F**, **Risler T**, **Ullrich S**, **Stefan N**, **Fritsche A**, **Haring HU.** Variance of the SGK1 gene is associated with insulin secretion in different European populations: results from the TUEF, EUGENE2, and METSIM studies. *PLoS One* 3: e3506, 2008.
19. **Schwab M**, **Lupescu A**, **Mota M**, **Mota E**, **Frey A**, **Simon P**, **Mertens PR**, **Floege J**, **Luft F**, **Asante-Poku S**, **Schaeffeler E**, **Lang F.** Association of SGK1 gene polymorphisms with type 2 diabetes. *Cell Physiol Biochem* 21: 151–160, 2008. doi:10.1159/000113757.
20. **Ackermann TF**, **Boini KM**, **Beier N**, **Scholz W**, **Fuchss T**, **Lang F.** EMD638683, a novel SGK inhibitor with antihypertensive potency. *Cell Physiol Biochem* 28: 137–146, 2011. doi:10.1159/000331722.
21. **Sierra-Ramos C**, **Velazquez-Garcia S**, **Vastola-Mascolo A**, **Hernández G**, **Faresse N**, **Alvarez de la Rosa D.** SGK1 activation exacerbates diet-induced obesity, metabolic syndrome and hypertension. *J Endocrinol* 244: 149–162, 2020. doi:10.1530/JOE-19-0275.
22. **Brunet A**, **Park J**, **Tran H**, **Hu LS**, **Hemmings BA**, **Greenberg ME.** Protein kinase SGK mediates survival signals by phosphorylating the forkhead transcription factor FKHRL1 (FOXO3a). *Mol Cell Biol* 21: 952–965, 2001. doi:10.1128/MCB.21.3.952-965.2001.
23. **Artunc F**, **Lang F.** Mineralocorticoid and SGK1-sensitive inflammation and tissue fibrosis. *Nephron Physiol* 128: 35–39, 2014. doi:10.1159/000368267.
24. **Quinkler M**, **Zehnder D**, **Eardley KS**, **Lepenies J**, **Howie AJ**, **Hughes SV**, **Cockwell P**, **Hewison M**, **Stewart PM.** Increased expression of mineralocorticoid effector mechanisms in kidney biopsies of patients with heavy proteinuria. *Circulation* 112: 1435–1443, 2005. doi:10.1161/CIRCULATIONAHA.105.539122.
25. **Artunc F**, **Amann K**, **Nasir O**, **Friedrich B**, **Sandulache D**, **Jahovic N**, **Risler T**, **Vallon V**, **Wulff P**, **Kuhl D**, **Lang F.** Blunted DOCA/high salt induced albuminuria and renal tubulointerstitial damage in gene-targeted mice lacking SGK1. *J Mol Med (Berl)* 84: 737–746, 2006. doi:10.1007/s00109-006-0082-0.
26. **Vallon V**, **Huang DY**, **Grahammer F**, **Wyatt AW**, **Osswald H**, **Wulff P**, **Kuhl D**, **Lang F.** SGK1 as a determinant of kidney function and salt intake in response to mineralocorticoid excess. *Am J Physiol Regul Integr Comp Physiol* 289: R395–R401, 2005. doi:10.1152/ajpregu.00731.2004.
27. **Shibata S**, **Nagase M**, **Yoshida S**, **Kawachi H**, **Fujita T.** Podocyte as the target for aldosterone: roles of oxidative stress and Sgk1. *Hypertension* 49: 355–364, 2007.
28. **Van Beusecum JP**, **Barbaro NR**, **McDowell Z**, **Aden LA**, **Xiao L**, **Pandey AK**, **Itani HA**, **Himmel LE**, **Harrison DG**, **Kirabo A.** High salt activates CD11c(+) antigen-presenting cells via SGK (serum glucocorticoid kinase) 1 to promote renal inflammation and salt-sensitive

hypertension. *Hypertension* 74: 555–563, 2019. doi:10.1161/HYPERTENSIONAHA.119.12761.

29. **Wu C**, **Yosef N**, **Thalhamer T**, **Zhu C**, **Xiao S**, **Kishi Y**, **Regev A**, **Kuchroo VK.** Induction of pathogenic TH17 cells by inducible salt-sensing kinase SGK1. *Nature* 496: 513–517, 2013. doi:10.1038/nature11984.
30. **Norlander AE**, **Saleh MA**, **Pandey AK**, **Itani HA**, **Wu J**, **Xiao L**, **Kang J**, **Dale BL**, **Goleva SB**, **Laroumanie F**, **Du L**, **Harrison DG**, **Madhur MS.** A salt-sensing kinase in T lymphocytes, SGK1, drives hypertension and hypertensive end-organ damage. *JCI Insight* 2, 2017. doi:10.1172/jci.insight.92801.
31. **Andres-Mateos E**, **Brinkmeier H**, **Burks TN**, **Mejias R**, **Files DC**, **Steinberger M**, **Soleimani A**, **Marx R**, **Simmers JL**, **Lin B**, **Finanger Hedderick E**, **Marr TG**, **Lin BM**, **Hourdé C**, **Leinwand LA**, **Kuhl D**, **Föller M**, **Vogelsang S**, **Hernandez-Diaz I**, **Vaughan DK**, **Alvarez de la Rosa D**, **Lang F**, **Cohn RD.** Activation of serum/glucocorticoid-induced kinase 1 (SGK1) is important to maintain skeletal muscle homeostasis and prevent atrophy. *EMBO Mol Med* 5: 80–91, 2013. doi:10.1002/emmm.201201443.
32. **Miranda P**, **Cadaveira-Mosquera A**, **Gonzalez-Montelongo R**, **Villarroel A**, **Gonzalez-Hernandez T**, **Lamas JA**, **Alvarez de la Rosa D**, **Giraldez T.** The neuronal serum- and glucocorticoid-regulated kinase 1.1 reduces neuronal excitability and protects against seizures through upregulation of the M-current. *J Neurosci* 33: 2684–2696, 2013.
33. **Hartner A**, **Cordasic N**, **Klanke B**, **Veelken R**, **Hilgers KF.** Strain differences in the development of hypertension and glomerular lesions induced by deoxycorticosterone acetate salt in mice. *Nephrol Dial Transplant* 18: 1999–2004, 2003. doi:10.1093/ndt/gfg299.
34. **Johns C**, **Gavras I**, **Handy DE**, **Salomao A**, **Gavras H.** Models of experimental hypertension in mice. *Hypertension* 28: 1064–1069, 1996. doi:10.1161/01.hyp.28.6.1064.
35. **Nakano D**, **Kwak CJ**, **Fujii K**, **Ikemura K**, **Satake A**, **Ohkita M**, **Takaoka M**, **Ono Y**, **Nakai M**, **Tomimori N**, **Kiso Y**, **Matsumura Y.** Sesamin metabolites induce an endothelial nitric oxide-dependent vasorelaxation through their antioxidative property-independent mechanisms: possible involvement of the metabolites in the antihypertensive effect of sesamin. *J Pharmacol Exp Ther* 318: 328–335, 2006.
36. **Luis-Lima S**, **Rodriguez-Rodriguez AE**, **Martin-Higueras C**, **Sierra-Ramos C**, **Carrara F**, **Arnau MR**, **Alvarez de la Rosa D**, **Salido E**, **Gaspari F**, **Porrini E.** Iohexol plasma clearance, a simple and reliable method to measure renal function in conscious mice. *Pflugers Arch* 468: 1587–1594, 2016.
37. **Ivy JR**, **Evans LC**, **Moorhouse R**, **Richardson RV**, **Al-Dujaili EAS**, **Flatman PW**, **Kenyon CJ**, **Chapman KE**, **Bailey MA.** Renal and Blood Pressure Response to a High-Salt Diet in Mice With Reduced Global Expression of the Glucocorticoid Receptor. *Front Physiol* 9: 848, 2018. doi:10.3389/fphys.2018.00848.
38. **Schindelin J**, **Arganda-Carreras I**, **Frise E**, **Kaynig V**, **Longair M**, **Pietzsch T**, **Preibisch S**, **Rueden C**, **Saalfeld S**, **Schmid B**, **Tinevez JY**, **White DJ**, **Hartenstein V**, **Eliceiri K**, **Tomancak P**, **Cardona A.** Fiji: an open-source platform for biological-image analysis. *Nat Methods* 9: 676–682, 2012. doi:10.1038/nmeth.2019.
39. **Garfield AS.** Derivation of primary mouse embryonic fibroblast (PMEF) cultures. *Methods Mol Biol* 633: 19–27, 2010.
40. **Penton D**, **Czogalla J**, **Wengi A**, **Himmerkus N**, **Loffing-Cueni D**, **Carrel M**, **Rajaram RD**, **Staub O**, **Bleich M**, **Schweda F**, **Loffing J.** Extracellular K(+) rapidly controls NaCl cotransporter phosphorylation in the native distal convoluted tubule by Cl(-) -dependent and independent mechanisms. *J Physiol* 594: 6319–6331, 2016.
41. **Carvalho BS**, **Irizarry RA.** A framework for oligonucleotide microarray preprocessing. *Bioinformatics* 26: 2363–2367, 2010. doi:10.1093/bioinformatics/btq431.
42. **Ritchie ME**, **Phipson B**, **Wu D**, **Hu Y**, **Law CW**, **Shi W**, **Smyth GK.** limma powers differential expression analyses for RNA-sequencing and microarray studies. *Nucleic Acids Res* 43: e47, 2015.
43. **Szklarczyk D**, **Gable AL**, **Lyon D**, **Junge A**, **Wyder S**, **Huerta-Cepas J**, **Simonovic M**, **Doncheva NT**, **Morris JH**, **Bork P**, **Jensen LJ**, **Mering CV.** STRING v11: protein-protein association networks with increased coverage, supporting functional discovery in genome-wide experimental datasets. *Nucleic Acids Res* 47: D607–D613, 2019. doi:10.1093/nar/gky1131.
44. **Shannon P**, **Markiel A**, **Ozier O**, **Baliga NS**, **Wang JT**, **Ramage D**, **Amin N**, **Schwikowski B**, **Ideker T.** Cytoscape: a software environment for integrated models of biomolecular interaction networks. *Genome Res* 13: 2498–2504, 2003. doi:10.1101/gr.1239303.
45. The Gene Ontology C. The Gene Ontology Resource: 20 years and still GOing strong. *Nucleic Acids Res* 47: D330–D338, 2019.
46. **Yu G**, **Wang LG**, **Han Y**, **He QY.** clusterProfiler: an R package for comparing biological themes among gene clusters. *OMICS* 16: 284–287, 2012.
47. **Schmittgen TD**, **Livak KJ.** Analyzing real-time PCR data by the comparative C(T) method. *Nat Protoc* 3: 1101–1108, 2008. doi:10.1038/nprot.2008.73.
48. **Hellemans J**, **Mortier G**, **De Paepe A**, **Speleman F**, **Vandesompele J.** qBase relative quantification framework and software for management and automated analysis of real-time quantitative PCR data. *Genome Biol* 8: R19, 2007. doi:10.1186/gb-2007-8-2-r19.
49. **Hernández-Díaz I**, **Giraldez T**, **Arnau MR**, **Smits VA**, **Jaisser F**, **Farman N**, **Alvarez de la Rosa D.** The mineralocorticoid receptor is a constitutive nuclear factor in cardiomyocytes due to hyperactive nuclear localization signals. *Endocrinology* 151: 3888–3899, 2010. doi:10.1210/en.2010-0099.
50. **Neris RLS**, **Dobles AMC**, **Gomes AV.** Western blotting using in-gel protein labeling as a normalization control: advantages of stain-free technology. *Methods Mol Biol* 2261: 443–456, 2021.
51. **Wyatt AW**, **Hussain A**, **Amann K**, **Klingel K**, **Kandolf R**, **Artunc F**, **Grahammer F**, **Huang DY**, **Vallon V**, **Kuhl D**, **Lang F.** DOCA-induced phosphorylation of glycogen synthase kinase 3beta. *Cell Physiol Biochem* 17: 137–144, 2006. doi:10.1159/000092075.
52. **Christensen BM**, **Perrier R**, **Wang Q**, **Zuber AM**, **Maillard M**, **Mordasini D**, **Malsure S**, **Ronzaud C**, **Stehle JC**, **Rossier BC**, **Hummler E.** Sodium and potassium balance depends on αENaC expression in connecting tubule. *J Am Soc Nephrol* 21: 1942–1951, 2010. doi:10.1681/ASN.2009101077.
53. **Vallon V**, **Wyatt AW**, **Klingel K**, **Huang DY**, **Hussain A**, **Berchtold S**, **Friedrich B**, **Grahammer F**, **Belaiba RS**, **Görlach A**, **Wulff P**, **Daut J**, **Dalton ND**, **Ross J Jr**, **Flögel U**, **Schrader J**, **Osswald H**, **Kandolf R**, **Kuhl D**, **Lang F.** SGK1-dependent cardiac CTGF formation and fibrosis following DOCA treatment. *J Mol Med (Berl)* 84: 396–404, 2006. doi:10.1007/s00109-005-0027-z.
54. **Cheng J**, **Truong LD**, **Wu X**, **Kuhl D**, **Lang F**, **Du J.** Serum- and glucocorticoid-regulated kinase 1 is upregulated following unilateral ureteral obstruction causing epithelial-mesenchymal transition. *Kidney Int* 78: 668–678, 2010. doi:10.1038/ki.2010.214.
55. **Schmidt-Ott KM**, **Mori K**, **Li JY**, **Kalandadze A**, **Cohen DJ**, **Devarajan P**, **Barasch J.** Dual action of neutrophil gelatinase-associated lipocalin. *J Am Soc Nephrol* 18: 407–413, 2007. doi:10.1681/ASN.2006080882.
56. **Eriksen BO**, **Stefansson VTN**, **Jenssen TG**, **Mathisen UD**, **Schei J**, **Solbu MD**, **Wilsgaard T**, **Melsom T.** Elevated blood pressure is not associated with accelerated glomerular filtration rate decline in the general non-diabetic middle-aged population. *Kidney Int* 90: 404–410, 2016. doi:10.1016/j.kint.2016.03.021.
57. **Hoy WE**, **Bertram JF**, **Denton RD**, **Zimanyi M**, **Samuel T**, **Hughson MD.** Nephron number, glomerular volume, renal disease and hypertension. *Curr Opin Nephrol Hypertens* 17: 258–265, 2008. doi:10.1097/MNH.0b013e3282f9b1a5.
58. **Sanchez OA**, **Ferrara LK**, **Rein S**, **Berglund D**, **Matas AJ**, **Ibrahim HN.** Hypertension after kidney donation: Incidence, predictors, and correlates. *Am J Transplant* 18: 2534–2543, 2018.
59. **Terada Y**, **Kuwana H**, **Kobayashi T**, **Okado T**, **Suzuki N**, **Yoshimoto T**, **Hirata Y**, **Sasaki S.** Aldosterone-stimulated SGK1 activity mediates profibrotic signaling in the mesangium. *J Am Soc Nephrol* 19: 298–309, 2008. doi:10.1681/ASN.2007050531.
60. **Han KH**, **Kang YS**, **Han SY**, **Jee YH**, **Lee MH**, **Han JY**, **Kim HK**, **Kim YS**, **Cha DR.** Spironolactone ameliorates renal injury and connective tissue growth factor expression in type II diabetic rats. *Kidney Int* 70: 111–120, 2006. doi:10.1038/sj.ki.5000438.
61. **Lijnen PJ**, **Petrov VV**, **Fagard RH.** Association between transforming growth factor-beta and hypertension. *Am J Hypertens* 16: 604–611, 2003. doi:10.1016/s0895-7061(03)00847-1.
62. **Murphy M**, **Godson C**, **Cannon S**, **Kato S**, **Mackenzie HS**, **Martin F**, **Brady HR.** Suppression subtractive hybridization identifies high glucose levels as a stimulus for expression of connective tissue growth

factor and other genes in human mesangial cells. *J Biol Chem* 274: 5830–5834, 1999.
63. **Lang F**, **Klingel K**, **Wagner CA**, **Stegen C**, **Warntges S**, **Friedrich B**, **Lanzendorfer M**, **Melzig J**, **Moschen I**, **Steuer S**, **Waldegger S**, **Sauter M**, **Paulmichl M**, **Gerke V**, **Risler T**, **Gamba G**, **Capasso G**, **Kandolf R**, **Hebert SC**, **Massry SG**, **Broër S.** Deranged transcriptional regulation of cell-volume-sensitive kinase hSGK in diabetic nephropathy. *Proc Natl Acad Sci U S A* 97: 8157–8162, 2000. doi:10.1073/pnas.97.14.8157.
64. **Gao S**, **Alarcón C**, **Sapkota G**, **Rahman S**, **Chen PY**, **Goerner N**, **Macias MJ**, **Erdjument-Bromage H**, **Tempst P**, **Massagué J.** Ubiquitin ligase Nedd4L targets activated Smad2/3 to limit TGF-beta signaling. *Mol Cell* 36: 457–468, 2009. doi:10.1016/j.molcel.2009.09.043.
65. **Kamenický P**, **Mazziotti G**, **Lombés M**, **Giustina A**, **Chanson P.** Growth hormone, insulin-like growth factor-1, and the kidney: pathophysiological and clinical implications. *Endocr Rev* 35: 234–281, 2014. doi:10.1210/er.2013-1071.
66. **Lother A**, **Fürst D**, **Bergemann S**, **Gilsbach R**, **Grahammer F**, **Huber TB**, **Hilgendorf I**, **Bode C**, **Moser M**, **Hein L.** Deoxycorticosterone acetate/salt-induced cardiac but not renal injury is mediated by endothelial mineralocorticoid receptors independently from blood pressure. *Hypertension* 67: 130–138, 2016. doi:10.1161/HYPERTENSIONAHA.115.06530.
67. **Gonzaga-Jauregui C**, **Gamble CN**, **Yuan B**, **Penney S**, **Jhangiani S**, **Muzny DM**, **Gibbs RA**, **Lupski JR**, **Hecht JT.** Mutations in COL27A1 cause Steel syndrome and suggest a founder mutation effect in the Puerto Rican population. *Eur J Hum Genet* 23: 342–346, 2015. doi:10.1038/ejhg.2014.107.
68. **Pace JM**, **Corrado M**, **Missero C**, **Byers PH.** Identification, characterization and expression analysis of a new fibrillar collagen gene. *Matrix Biol* 22: 3–14, 2003.
69. **Atkinson JM**, **Pullen N**, **Da Silva-Lodge M**, **Williams L**, **Johnson TS.** Inhibition of Thrombin-Activated Fibrinolysis Inhibitor Increases Survival in Experimental Kidney Fibrosis. *J Am Soc Nephrol* 26: 1925–1937, 2015. doi:10.1681/ASN.2014030303.
70. **Karsdal MA**, **Nielsen SH**, **Leeming DJ**, **Langholm LL**, **Nielsen MJ**, **Manon-Jensen T**, **Siebuhr A**, **Gudmann NS**, **Rønnow S**, **Sand JM**, **Daniels SJ**, **Mortensen JH**, **Schuppan D.** The good and the bad collagens of fibrosis - Their role in signaling and organ function. *Adv Drug Deliv Rev* 121: 43–56, 2017. doi:10.1016/j.addr.2017.07.014.
71. **Merline R**, **Lazaroski S**, **Babelova A**, **Tsalastra-Greul W**, **Pfeilschifter J**, **Schluter KD**, **Gunther A**, **Iozzo RV**, **Schaefer RM**, **Schaefer L.** Decorin deficiency in diabetic mice: aggravation of nephropathy due to overexpression of profibrotic factors, enhanced apoptosis and mononuclear cell infiltration. *J Physiol Pharmacol* 60: 5–13, 2009.
72. **Ferdous Z**, **Wei VM**, **Iozzo R**, **Höök M**, **Grande-Allen KJ.** Decorin-transforming growth factor- interaction regulates matrix organization and mechanical characteristics of three-dimensional collagen matrices. *J Biol Chem* 282: 35887–35898, 2007. doi:10.1074/jbc.M705180200.
73. **Tan RJ**, **Liu Y.** Matrix metalloproteinases in kidney homeostasis and diseases. *Am J Physiol Renal Physiol* 302: F1351–1361, 2012. doi:10.1152/ajprenal.00037.2012.
74. **Zakiyanov O**, **Kalousová M**, **Zima T**, **Tesarõ V.** Matrix metalloproteinases in renal diseases: a critical appraisal. *Kidney Blood Press Res* 44: 298–330, 2019. doi:10.1159/000499876.
75. **Regos E**, **Abdelfattah HH**, **Reszegi A**, **Szilak L**, **Werling K**, **Szabo G**, **Kiss A**, **Schaff Z**, **Kovalszky I**, **Baghy K.** Syndecan-1 inhibits early stages of liver fibrogenesis by interfering with TGFbeta1 action and upregulating MMP14. *Matrix Biol*: 68–69474: –489, 2018. doi:10.1016/j.matbio.2018.02.008.
76. **Zigrino P**, **Brinckmann J**, **Niehoff A**, **Lu Y**, **Giebeler N**, **Eckes B**, **Kadler KE**, **Mauch C.** Fibroblast-derived MMP-14 regulates collagen homeostasis in adult skin. *J Invest Dermatol* 136: 1575–1583, 2016. doi:10.1016/j.jid.2016.03.036.
77. **Chen W**, **Yang A**, **Jia J**, **Popov YV**, **Schuppan D**, **You H.** Lysyl oxidase (LOX) family members: rationale and their potential as therapeutic targets for liver fibrosis. *Hepatology* 72: 729–741, 2020. doi:10.1002/hep.31236.
78. **Cosgrove D**, **Dufek B**, **Meehan DT**, **Delimont D**, **Hartnett M**, **Samuelson G**, **Gratton MA**, **Phillips G**, **MacKenna DA**, **Bain G.** Lysyl oxidase like-2 contributes to renal fibrosis in Col4α3/Alport mice. *Kidney Int* 94: 303–314, 2018. doi:10.1016/j.kint.2018.02.024.
79. **Xu XH**, **Jia Y**, **Zhou X**, **Xie D**, **Huang X**, **Jia L**, **Zhou Q**, **Zheng Q**, **Zhou X**, **Wang K**, **Jin LP.** Downregulation of lysyl oxidase and lysyl oxidase-like protein 2 suppressed the migration and invasion of trophoblasts by activating the TGF-β/collagen pathway in preeclampsia. *Exp Mol Med* 51: 1–12, 2019. doi:10.1038/s12276-019-0211-9.
80. **Nakasaki M**, **Hwang Y**, **Xie Y**, **Kataria S**, **Gund R**, **Hajam EY**, **Samuel R**, **George R**, **Danda D**, **Jp M**, **Nakamura T**, **Shen Z**, **Briggs S**, **Varghese S**, **Jamora C.** The matrix protein Fibulin-5 is at the interface of tissue stiffness and inflammation in fibrosis. *Nat Commun* 6: 8574, 2015.
81. **Taguchi T**, **Razzaque MS.** The collagen-specific molecular chaperone HSP47: is there a role in fibrosis? *Trends Mol Med* 13: 45–53, 2007. doi:10.1016/j.molmed.2006.12.001.
82. **Shao Z**, **Nishimura T**, **Leung LL**, **Morser J.** Carboxypeptidase B2 deficiency reveals opposite effects of complement C3a and C5a in a murine polymicrobial sepsis model. *J Thromb Haemost* 13: 1090–1102, 2015. doi:10.1111/jth.12956.
83. **Yoshida T**, **Kato K**, **Fujimaki T**, **Yokoi K**, **Oguri M**, **Watanabe S**, **Metoki N**, **Yoshida H**, **Satoh K**, **Aoyagi Y**, **Nishigaki Y**, **Tanaka M**, **Nozawa Y**, **Yamada Y.** Association of a polymorphism of the apolipoprotein E gene with chronic kidney disease in Japanese individuals with metabolic syndrome. *Genomics* 93: 221–226, 2009. doi:10.1016/j.ygeno.2008.11.001.
84. **Borel F**, **Sun H**, **Zieger M**, **Cox A**, **Cardozo B**, **Li W**, **Oliveira G**, **Davis A**, **Gruntman A**, **Flotte TR**, **Brodsky MH**, **Hoffman AM**, **Elmallah MK**, **Mueller C.** Editing out five Serpina1 paralogs to create a mouse model of genetic emphysema. *Proc Natl Acad Sci U S A* 115: 2788–2793, 2018. doi:10.1073/pnas.1713689115.
85. **Fischer HP**, **Ortiz-Pallardó ME**, **Ko Y**, **Esch C**, **Zhou H.** Chronic liver disease in heterozygous alpha1-antitrypsin deficiency PiZ. *J Hepatol* 33: 883–892, 2000. doi:10.1016/S0168-8278(00)80119-1.
86. **Maicas N**, **van der Vlag J**, **Bublitz J**, **Florquin S**, **Bakker-van Bebber M**, **Dinarello CA**, **Verweij V**, **Masereeuw R**, **Joosten LA**, **Hilbrands LB.** Human Alpha-1-Antitrypsin (hAAT) therapy reduces renal dysfunction and acute tubular necrosis in a murine model of bilateral kidney ischemia-reperfusion injury. *PLoS One* 12: e0168981, 2017. doi:10.1371/journal.pone.0168981.
87. **Latouche C**, **Sainte-Marie Y**, **Steenman M**, **Castro Chaves P**, **Naray-Fejes-Toth A**, **Fejes-Toth G**, **Farman N**, **Jaisser F.** Molecular signature of mineralocorticoid receptor signaling in cardiomyocytes: from cultured cells to mouse heart. *Endocrinology* 151: 4467–4476, 2010. doi:10.1210/en.2010-0237.
88. **Sánchez-Navarro A**, **Mejía-Vilet JM**, **Pérez-Villalva R**, **Carrillo-Pérez DL**, **Marquina-Castillo B**, **Gamba G**, **Bobadilla NA.** serpina3 in the early recognition of acute kidney injury to chronic kidney disease (CKD) transition in the rat and its potentiality in the recognition of patients with CKD. *Sci Rep* 9: 10350, 2019. doi:10.1038/s41598-019-46601-1.
89. **Eksteen B**, **Miles A**, **Curbishley SM**, **Tselepis C**, **Grant AJ**, **Walker LS**, **Adams DH.** Epithelial inflammation is associated with CCL28 production and the recruitment of regulatory T cells expressing CCR10. *J Immunol* 177: 593–603, 2006. doi:10.4049/jimmunol.177.1.593.
90. **Cippà PE**, **Liu J**, **Sun B**, **Kumar S**, **Naesens M**, **McMahon AP.** A late B lymphocyte action in dysfunctional tissue repair following kidney injury and transplantation. *Nat Commun* 10: 1157, 2019. doi:10.1038/s41467-019-09092-2.
91. **Mattson DL.** Infiltrating immune cells in the kidney in salt-sensitive hypertension and renal injury. *Am J Physiol Renal Physiol* 307: F499–508, 2014.
92. **Bubb KJ**, **Khambata RS**, **Ahluwalia A.** Sexual dimorphism in rodent models of hypertension and atherosclerosis. *Br J Pharmacol* 167: 298–312, 2012. doi:10.1111/j.1476-5381.2012.02036.x.
93. **Karatas A**, **Hegner B**, **de Windt LJ**, **Luft FC**, **Schubert C**, **Gross V**, **Akashi YJ**, **Gürgen D**, **Kintscher U**, **da Costa Goncalves AC**, **Regitz-Zagrosek V**, **Dragun D.** Deoxycorticosterone acetate-salt mice exhibit blood pressure-independent sexual dimorphism. *Hypertension* 51: 1177–1183, 2008. doi:10.1161/HYPERTENSIONAHA.107.107938.